Engineering Structures 345 (2025) 121461

Contents lists available at ScienceDirect

Engineering Structures

journal homepage: www.elsevier.com/locate/engstruct

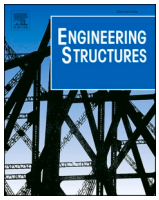

Life-cycle environmental impact optimization of an RC-THVS composite frame for sustainable construction

Iván Negrin [a,*,1], Moacir Kripka [b,2], Víctor Yepes [a,3]

[a] Institute of Concrete Science and Technology (ICITECH), Universitat Politècnica de València, Valencia 46022, Spain
[b] Civil Engineering Graduate Program, Federal University of Technology-Paraná, Via do Conhecimento, Km 1, Pato Branco, Paraná 85503-390, Brazil

ARTICLE INFO

Keywords:
Life-Cycle Environmental Impact Optimization,
reinforced concrete
Hybrid steel girder
Tapered girder
Frame building
Global Warming Potential

ABSTRACT

This study investigates the benefits of Life-Cycle Environmental Impact Optimization (LCEIO) in structural engineering, focusing on the RC-THVS composite typology as a sustainable alternative for frame-building construction. This innovative structural system integrates reinforced concrete (RC) columns with Transversely Hybrid Variable Section (THVS) steel girders serving as beam elements. The optimization problem is formulated to optimize the Global Warming Potential of the building structure during its life cycle. A novel LHS-CINS algorithm is introduced to solve the formulated optimization problems efficiently. Results show that LCEIO reduces environmental impact significantly, with optimized structures achieving up to a 32 % reduction in emissions compared to traditionally designed buildings. The most substantial improvement occurs in the manufacturing phase, where THVS girders lower emissions by up to 70 % compared to traditional I-section profiles. Additionally, maintenance-related impacts decrease by 45 % due to the girders' optimized tapered geometry. When comparing optimized solutions, rigid-joint composite typologies outperform RC systems in low-aggressiveness environments, reducing life-cycle emissions by 30 %. In highly aggressive environments, composite structures remain more sustainable than RC ones, although maintenance impacts are accentuated. Beyond individual component performance, THVS girders contribute to overall structural efficiency by reducing self-weight, thereby lowering axial loads on columns and foundations. Moreover, when slabs and walls are integrated into the superstructure, composite typologies further enhance system efficiency, cutting emissions by up to 42 % compared to bare frame models. The findings emphasize the capability of LCEIO and composite configurations to design more sustainable, efficient, and environmentally responsible building solutions.

1. Introduction

As a major contributor to environmental degradation, the construction industry demands transformation to meet sustainability goals. Efforts to mitigate its impact include developing low-carbon materials and strategies to optimize material use. Structural optimization supports this by automating design to control material type and quantity, fostering innovative typologies aligned with Modern Methods of Construction [1].

Reinforced concrete (RC) frames dominate building typologies, prompting initial research on economic optimization of realistic 3D structures [2,3]. Environmental objectives have gained traction, with studies targeting CO_2 reduction in varied contexts, including low- and mid-rise buildings [4], prefabricated systems [5], modular construction integrating BIM-based design [6], and building models that incorporate soil-structure interaction [7]. Embodied emission metrics have proven valuable for impact assessment [8], while multi-objective approaches now integrate cost with constructability [9] and durability [10]. Several studies have also explored the role of structural optimization in enhancing progressive collapse resistance in RC buildings [11,12]. While these advances are significant, most applications focus on conventional RC systems and early design stages, with limited attention to innovative typologies such as hybrid or composite systems. Moreover, early-stage metrics often overlook long-term performance, emphasizing the need for optimization frameworks that integrate emerging typologies with full life-cycle assessment.

* Corresponding author.
E-mail address: ianegdia@doctor.upv.es (I. Negrin).
[1] 0000–0002-0304–5621
[2] 0000–0002-1997–3414
[3] 0000–0001-5488–6001

https://doi.org/10.1016/j.engstruct.2025.121461
Received 21 June 2025; Received in revised form 9 September 2025; Accepted 24 September 2025
Available online 29 September 2025

Nomenclature

A	Exposed concrete surface area
BBO	Biogeography-Based Optimization
b_f	Girder flange width
BF	Bare frame
c	Cement content per m^3 of concrete
CINS	Constrained Iterative Neighborhood Sampling
cs	Soil cohesion
CS-1, 2, 3	Case studies 1, 2, and 3
CaO	Calcium oxide content in cement
Comp F	Composite typology with fixed joints
Comp P	Composite typology with pinned joints
d	Concrete cover thickness
D	Modulus of elasticity of the soil
E	Modulus of elasticity of the soil
$elca_j$	Unit environmental impact of each process
Fx	Dimension in the direction of the x-axis of the foundation base
Fy	Dimension in the direction of the y-axis of the foundation base
f_{yf}	Steel yield strength of the flanges
f_{yw}	Steel yield strength of the web
GWP	Global Warming Potential
HFS	High-Fidelity Simulations
IF	Integrated frame
k	Carbonation rate coefficient
ks	Soil stiffness coefficient
L	Beam-type element span
L_i	Live load
L/d	Length (span) to depth ratio in girders
LCA	Life-Cycle Analysis
LCEIO	Life-Cycle Environmental Impact Optimization
LCI	Life Cycle Inventory
LHS	Latin Hypercube Sampling
M	Chemical molar fraction
m_j	Measure that quantifies each process
n	Solutions that improve upon the basic one
N	Set of initial LHS solutions
OD	Optimized design
p	Pressure acting on the foundation base
P	Coating system's practical service life
$q^*_{br\_II}$	Foundation base bearing capacity pressure
r	Proportion of CaO that can be carbonated
R'^*	Linearity limit stress of the soil
RC	Reinforced concrete
R_h	Hybrid ratio
S	Foundation base settlement
$\overline{S}$	Foundation base settlement for an acting pressure equal to the base linearity limit stress of the soil
SL	Service life
SSI	Soil-Structure Interaction
TD	Traditional design
t_f	Girder flange thickness
THVS	Transversely Hybrid Variable Section
TP	Transition point
t_w	Girder web thickness
v_c	Corrosion rate
xi	Design variables
W	Wind load
ϕ	Soil friction angle
γ	Soil density

Composite structures, which integrate multiple materials within a single system, offer a promising route to enhance structural performance and sustainability. Numerous studies highlight their advantages across diverse applications. Hassan et al. (2024) [13] developed eco-friendly steel-concrete-steel composites incorporating polypropylene fibers and ground granulated blast-furnace slag, achieving improved ductility, tensile strength, and reduced environmental impact. Lee et al. (2016) [14] reported that steel-concrete frames significantly lower embodied emissions in long-span and heavy-load buildings, compared to RC. Environmental Life-Cycle Analysis (LCA) has supported these findings, as shown in Brambilla et al. (2019) [15] for composite floor systems. Other innovations include Amin et al. (2025) [16], who applied engineered cementitious composites and bamboo reinforcement for deep beams with large openings, achieving accurate shear performance predictions and sustainability gains. Sabsabi et al. (2025) [17] demonstrated that externally prestressed curved composite beams improve moment capacity, deflection control, and material efficiency. These studies collectively illustrate how strategic material integration in composites leads to more efficient and environmentally responsible structural systems.

However, despite the well-established benefits of composite systems, their integration with optimization techniques in building design processes has been limited [18]. Paksoy et al. (2024) [19] optimized composite columns, achieving superior cost efficiency compared to traditional systems. Similarly, Shu et al. (2025) [20] applied a multi-objective optimization framework to timber–concrete hybrids, showing that replacing conventional members with innovative alternatives can substantially reduce carbon emissions while maintaining structural performance, thereby enhancing the sustainability of structural systems. Mela and Heinisuo (2014) [21] applied optimization to hybrid steel I-girders, revealing that mixed-material configurations are more cost-effective than homogeneous ones. Negrin et al. (2023c) [22] further refined optimization methods by enhancing the hybrid ratio (R_h), which defines the strength balance between flange and web steels [23]. Their findings show that R_h values between 1.70 and 2.00 lead to up to 20 % cost savings. Initially intended for long-span structures such as bridges, these hybrid girders also demonstrate promising applicability in building structures. Still, existing optimization studies on composite/hybrid elements often address simplified scenarios, focusing on isolated components and neglecting long-term, life-cycle performance.

Minimizing structural weight is another key strategy for reducing a building's environmental impact, as it directly affects material use and embodied emissions. Machado et al. (2025) [24] analyzed mid- and high-rise buildings, showing that lighter systems, such as those using timber or hybrid materials, can significantly lower embodied greenhouse gas emissions. Yet, these insights are often not fully integrated into comprehensive design optimization frameworks. Advancing lighter structural systems therefore requires optimization methods that simultaneously enhance environmental performance and maintain structural efficiency.

In response to this need for integrated optimization, some recent studies have used this tool to investigate composite typologies that improve both structural efficiency and material use. An innovative strategy involves combining transversely hybrid variable section (THVS) girders into frame-building construction, as proposed by Negrin et al. (2025b) [25]. These girders merge hybrid material configurations with variable cross-sections to align with internal force distributions, particularly bending moments. Combined with RC columns, the system leverages the horizontal stiffness of concrete elements and structural steel's reduced weight and adaptability. Unlike conventional steel

frames, this composite typology eliminates the need for shear walls in low- and mid-rise buildings, reducing material use while preserving efficiency. The lighter THVS girders also lower axial loads on columns and foundations, optimizing structural and environmental performance. Compared to optimized RC frames, this configuration can reduce embodied emissions and energy use by over 15 % [25]. While these results are promising, they are based on cradle-to-gate assessments, omitting critical life-cycle stages such as service performance, maintenance, and end-of-life processes, highlighting the need for full life-cycle evaluation to quantify long-term sustainability benefits accurately.

Recent advances have underscored the importance of life-cycle thinking in structural design. Ping et al. (2024) [26] presented a comprehensive framework for assessing life-cycle carbon emissions in steel frames exposed to seismic hazards, demonstrating that self-centering braced frames (SCBFs) can reduce total emissions by up to 14.6 % over 100 years, mainly by limiting post-earthquake residual deformations. In a follow-up study, Ping et al. (2025) [27] introduced a life-cycle cost framework that combines seismic loss and environmental costs. Their results confirmed that although SCBFs have higher upfront impacts, they significantly reduce seismic-related emissions (up to 61.6 %) and total life-cycle losses compared to conventional systems. These studies highlight the potential of integrating seismic resilience and environmental impact assessments over the building's full life span through probabilistic frameworks that account for uncertainty. Other research has also contributed valuable insights into the benefits of LCA. Fan et al. (2024) [28] demonstrated that using ultra-high-performance concrete (UHPC) beams can lower life-cycle emissions by over 25 %, with full UHPC use reaching up to 48 % savings. Wang et al. (2025) [29] incorporated climate-induced degradation into maintenance modeling, emphasizing how time-dependent deterioration affects environmental performance. Although these studies demonstrate the value of LCA in guiding material choices and assessing long-term impacts, they do not systematically integrate optimization strategies into the design process, limiting their ability to enhance structural and environmental outcomes.

To address this limitation, Life-Cycle Environmental Impact Optimization (LCEIO) emerges as a more advanced approach, actively integrating optimization techniques to improve both structural and environmental outcomes across all stages of the building's life cycle. Heydari and Heravi (2023) [30] demonstrated that simultaneously optimizing embodied and operational carbon can reduce emissions by nearly 25 % while improving cost efficiency. Su et al. (2023) [31] introduced a dynamic LCA model that incorporates time-varying impacts, and Chen et al. (2025) [32] combined LCA with machine learning and spatial modeling to identify key emission drivers. Gao et al. (2025) [33] proposed an AI-driven generative design method that enhances life-cycle cost, energy use, and efficiency, emphasizing the role of optimization in achieving sustainable design. Despite these promising developments, several limitations remain unaddressed. Many studies rely on simplified case studies that exclude critical components such as foundations and their interaction with the underlying terrain, overlooking the role of Soil-Structure Interaction (SSI) in life-cycle performance. Additionally, the proposed optimization methods often require many simulations, which can limit the analysis of multiple typologies across different case studies, especially when the structural models involved are computationally expensive.

This study seeks to overcome the above limitations and, based on the work of Negrin et al. (2025b) [25], applies a LCEIO framework to both a novel RC–THVS composite typology and a conventional RC frame, enabling a direct and robust comparison of their long-term performance. Unlike previous research focused primarily on early design stages, this study evaluates structural and environmental behavior over the entire life cycle, including material aging, scheduled maintenance, and end-of-life scenarios. It also accounts for varying environmental conditions, allowing for a realistic analysis of performance across diverse geographic contexts. A notable advancement of this study is the integration of SSI, a critical yet often neglected factor that can significantly affect durability predictions and maintenance accuracy. To address the high computational cost typically associated with evaluating multiple typologies across various case studies using complex High-Fidelity Simulations (HFS), this study introduces a novel and efficient optimization algorithm. The proposed method significantly improves convergence speed while preserving predictive accuracy, making it feasible to explore and compare alternative structural solutions at a realistic scale. By enabling LCA and optimization of innovative composite systems under detailed and practical modeling conditions, this approach directly tackles key limitations in current research and offers a scalable, efficient strategy for sustainable structural design.

2. Methodology

2.1. Structural systems and design considerations

This study evaluates a novel composite structural system, RC-THVS, as an alternative to conventional monolithic RC frames. The RC-THVS typology integrates RC columns and foundations with specialized steel THVS girders, tapered I-section hybrid elements specifically designed to maximize structural efficiency. Unlike conventional composite systems, which often rely on standard steel profiles combined with concrete slabs to achieve composite action, the proposed system introduces a customized hybrid steel element as a core structural component. Combining both materials' advantages in a system-level configuration, the RC-THVS typology seeks to enhance structural performance while minimizing environmental impact and resource consumption [25].

As illustrated at the top of Fig. 1, three case studies of buildings are implemented to evaluate the performance of the structural typologies (bottom Fig. 1). In all cases, the superstructure consists exclusively of frame elements. Slabs and walls are assumed to provide no structural contribution. Their effect is considered only as dead load within the analysis. In the traditional typology, all element connections are considered fixed. In contrast, the composite typology introduces two connection variants: fixed and pinned. An essential aspect of the study is the explicit consideration of foundation design as an integral component of the structural framework. The interaction between the foundations and the underlying soil is incorporated into the modeling to capture real-world structural behavior accurately.

The building system's structural modeling, analysis, and design uses SAP2000, a widely validated tool for advanced structural simulations. In the case of THVS girders, SAP2000 enables an accurate representation of their behavior under both support configurations considered. Although the software does not perform direct design checks for such hybrid elements, it allows for the extraction of internal forces, which are then processed through a custom MATLAB routine that verifies compliance with all relevant design constraints based on the methodology proposed by [22], as detailed in the Constraints section.

The structural design of RC elements is carried out using the Limit State Method by the ACI 318–19 code. The main load combinations considered in the analysis are given in Eqs. 1–4, where D, L_i, and W denote dead, live, and extreme wind loads, respectively. These load values are summarized in Table 1. Additional combinations are evaluated for foundation design and to verify compliance with serviceability limit states. For a detailed description of the structural modeling approach, consult [7].

$$1.2 \bullet D + 1.6 \bullet L_i \tag{1}$$

$$1.2 \bullet D + 0.8 \bullet W \tag{2}$$

$$1.2 \bullet D + 1.4 \bullet W + 0.5 \bullet L_i \tag{3}$$

$$0.9 \bullet D + 1.4 \bullet W \tag{4}$$

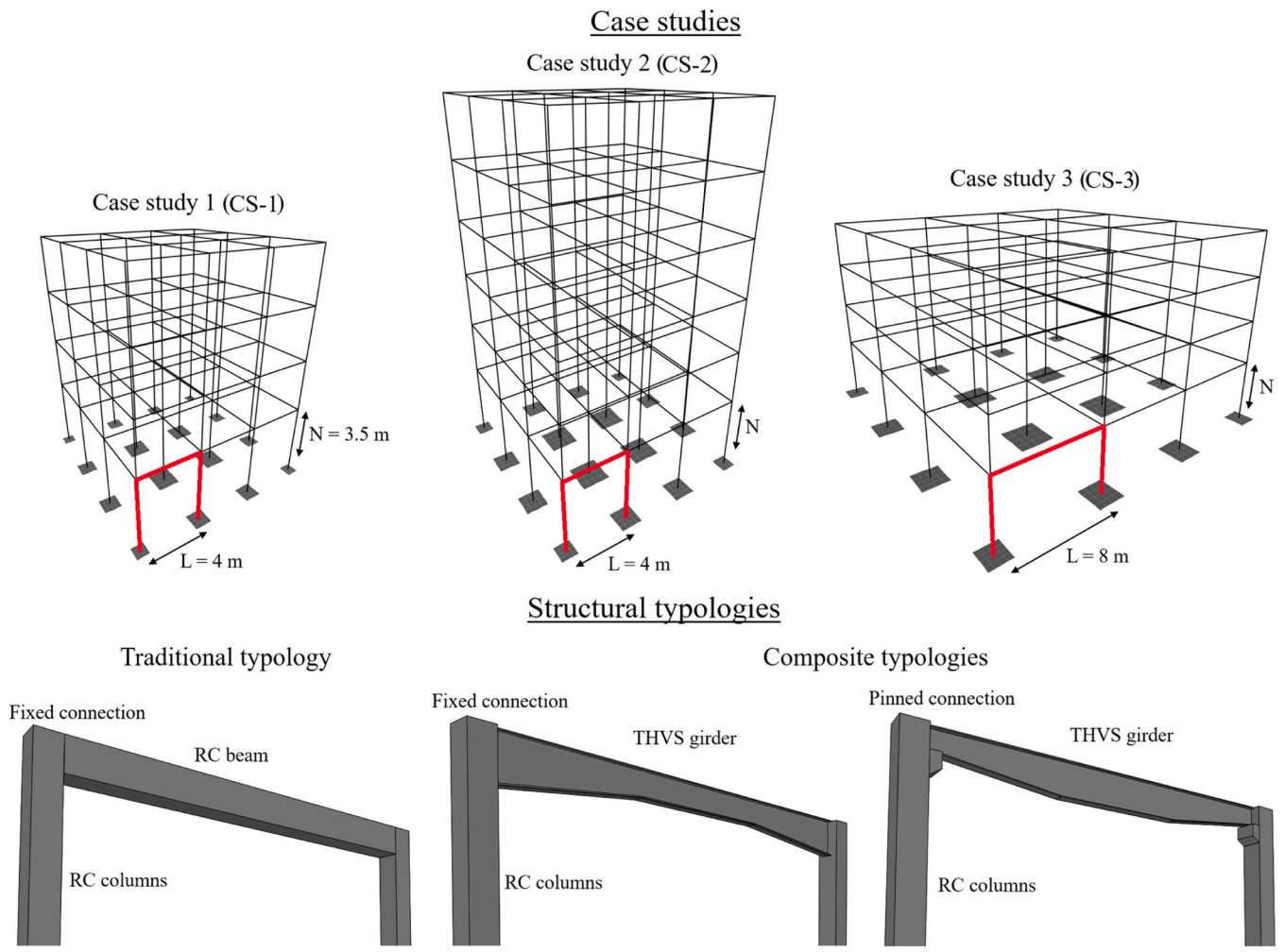

Fig. 1. Top: three case studies. Bottom: Three typologies to be optimized using the three case studies.

Table 1
Loads considered.

Description	Value	
Dead load on lower floors	4.80 kN/m^2	
Dead load on roof	5.40 kN/m^2	
Live load on lower floors (Offices)	3.00 kN/m^2	
Live load on roof	0.80 kN/m^2	
Extreme wind load	Positive pressure	Negative pressure
	0.92 kN/m^2 0–5 m,	0.50 kN/m^2 0–5 m,
	1.01 kN/m^2 at 7 m,	0.55 kN/m^2 at 7 m,
	1.13 kN/m^2 at	0.62 kN/m^2 at
	10.5 m,	10.5 m,
	1.25 kN/m^2 at 14 m,	0.69 kN/m^2 at 14 m,
	1.37 kN/m^2 at	0.76 kN/m^2 at
	17.5 m,	17.5 m,
	1.50 kN/m^2 at 21 m.	0.83 kN/m^2 at 21 m.

2.1.1. Soil-structure interaction model

Given the intricate nature of its modeling, SSI is frequently disregarded in optimization studies. However, its inclusion can markedly affect the behavior of the superstructure and, consequently, alter key aspects of the design. Prior studies have demonstrated that neglecting SSI can lead to material quantity discrepancies of up to 20 % in superstructure design [7]. The prevailing assumption behind this effect is that designs based on idealized fixed supports tend to be underdesigned, requiring less material compared to those that account for foundation flexibility and soil interaction. This difference stems from differential settlements between neighboring foundations, which arise due to variations in geometry and applied loads. Even when these settlements remain within acceptable thresholds, they introduce additional stresses into the superstructure, particularly by increasing bending effects relative to a system with rigid supports. SSI is integrated through a local Winkler-type deformation model, in which the soil stiffness coefficient (ks) is determined by correlating the applied pressure (p) with the resulting settlement (S).

To account for the limited depth of compressible soil, the subgrade is modeled as a linearly elastic half-space, as illustrated in Fig. 2(a). The foundation is treated as a shallow slab footing, and its interaction with the supporting soil is defined through a pressure–settlement response, which serves to quantify soil stiffness. This modeling approach has been supported by various studies conducted under differing geotechnical conditions [34]. The pressure–settlement relationship is formulated using the curve proposed by Klepikov (1969) [35], presented in Eq. 5. In this formulation, $\overline{S}$ denotes the settlement corresponding to an applied pressure equal to the soil's base linearity limit stress R'^*, while $q^*_{br\_II}$ represents the ultimate bearing pressure, derived from principles of plasticity theory. The methodology adopted for integrating SSI within the optimization process is outlined in Fig. 2(b).

$$ks = \frac{p}{S} = \frac{q^*_{br\_II} - p}{\overline{S} \cdot \left[\left(\frac{q^*_{br\_II}}{R'^*}\right) - 1\right]} \quad \left(\frac{kN/m^2}{m}\right) \tag{5}$$

The soil properties assumed in this study are as follows: modulus of elasticity (E) = 12,000 kPa, Poisson's ratio (μ) = 0.40, cohesion (cs)

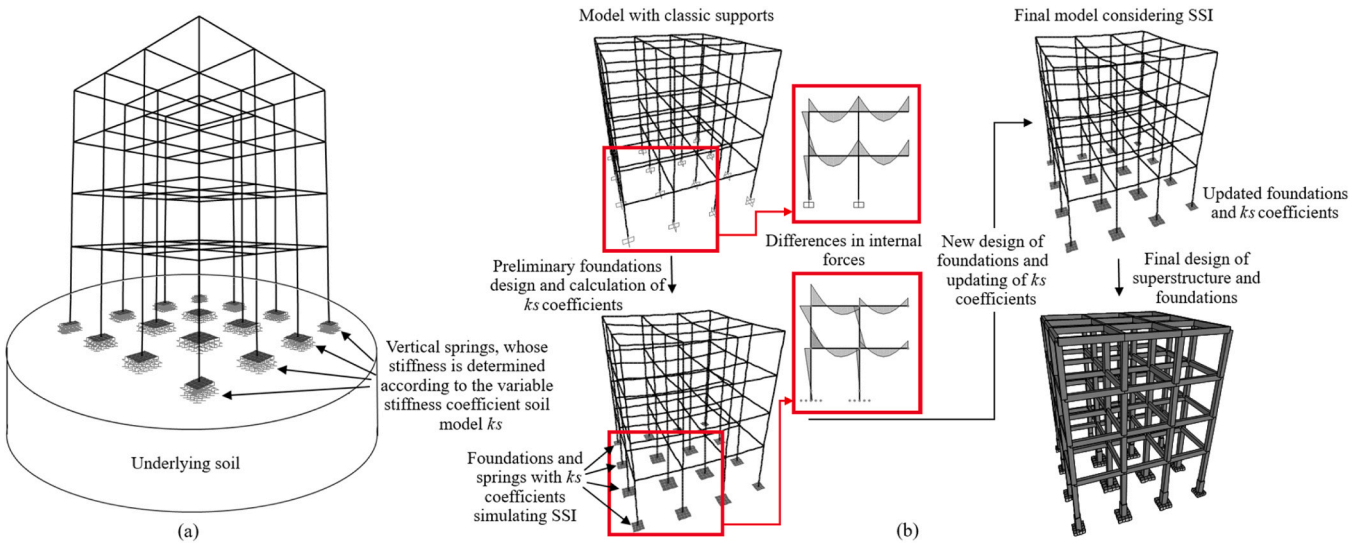

Fig. 2. (a) Overview of the SSI modeling approach, (b) schematic representation of the procedure for automatic integration of SSI into the optimization-based framework. For more information, refer to [7].

$= 60$ kPa, friction angle (ϕ) $= 8°$, and density (γ) $= 19$ kN/m^3. For further details on this methodology, refer to [7].

2.2. Life-cycle environmental impact optimization problem formulation

2.2.1. Objective function

The optimization problem's objective function is the building's environmental impact. This impact is assessed over the buildings' entire lifespan using Life-Cycle Assessment (LCA), a standardized methodology [36] that systematically considers all inputs (resources, energy) and outputs (emissions, waste) of a system, making it a valuable tool for sustainability studies in construction [37,38].

To ensure a fair comparison, all structural systems are designed with equivalent functional parameters, such as building geometry parameters (see case studies in Fig. 1) and a lifespan of 100 years. The environmental impact is analyzed under two distinct exposure conditions: one corresponding to a low-aggressiveness environment with moderate humidity and another representing a high-aggressiveness marine environment.

The Life Cycle Inventory (LCI) quantifies all inputs and outputs in the system, using data sources such as Ecoinvent v3.7.1, BEDEC (2016) [39], and scientific literature. GreenDelta's OpenLCA software is used to model the life cycle [40]. The ReCiPe midpoint approach is employed, with Global Warming Potential (GWP, kg CO_2 eq) selected as the primary impact indicator. This indicator has proven to be an excellent metric for evaluating the impact of building construction [8].

Mathematically, Eq. 6 defines the objective function that is minimized in the optimization process. Here, i represents each life cycle stage, and j represents each process associated with a specific stage (see Fig. A.1 in Appendix). On the other hand, $elca_j$ represents the unit environmental impact of each process (see Table A.1 in Appendix A), while m_j is the measure that quantifies the process.

$$GWP = \sum_{i=1}^{n}\sum_{j=1}^{p} elca_j \bullet m_j \quad (kgCO_2eq) \tag{6}$$

2.2.1.1. Life-cycle assessment methodology. The system boundary of the LCA includes four key life cycle stages: manufacturing, construction, use and maintenance, and end-of-life. Each phase contributes to the overall environmental impact. Fig. A.1 in Appendix A summarizes the key considerations addressed at each LCA stage.

The manufacturing phase involves transforming raw materials into products needed for constructing the building. For RC elements, concrete production includes the acquisition/production of raw materials (sand, aggregate, cement, and similar), followed by their transportation over 100 km to the mixing plant, where they are combined to produce concrete. The production of reinforcing steel involves a similar transportation process, with raw materials traveling 100 km before being processed into reinforcement bars.

For THVS girders, steel production is carried out using a combination of Electric Arc Furnace (EAF) and Basic Oxygen Furnace (BOF) processes. Lower-quality steels contain up to 100 % recycled content, whereas higher-quality steels rely more on virgin iron ore, with a 15–30 % recycled content. The Ecoinvent v3.7.1 database provides baseline data for S235-grade steel. The indicators of other steel grades are obtained from this basic value using data from [41] (see Table A.1 in Appendix A). Fabrication activities also generate environmental burdens. Cutting [42], welding, and painting impacts are shown in Table A.1 in Appendix A. Painting using spraying machine results in 0.08 kg CO_2 eq per square meter of painted surface for a single coat of Alkyd paint. The energy consumption of the spraying machine is 1.5 kWh per square meter, translating to an additional 0.61 kg CO_2 eq [43].

The construction phase includes transporting materials over 100 km and the energy consumption of construction equipment. Concrete handling requires 123.42 MJ of energy, leading to 62.79 kg CO_2 eq emissions per cubic meter [39]. The processing of reinforcing steel requires 10.2 MJ per kilogram, which results in emissions of 0.94 kg CO_2 eq per kilogram of steel [39]. The production and installation of formwork contribute 2.53 kg CO_2 eq per square meter [39].

The THVS girder manufacturing also involves emissions from transportation and installation activities. The energy required for the erection of girders is estimated at 0.019 kWh per minute of effective operation time, which results in an emission of 0.009 kg CO_2 eq [44].

The foundation work contributes additional emissions due to excavation and backfilling processes, which generate 0.52 kg CO_2 eq per cubic meter of soil excavated or backfilled. The total volume affected is determined by the foundation design (see excavation scheme in Fig. 3).

The use and maintenance phase is defined by a maintenance strategy that depends on environmental conditions. Preventive measures are implemented to ensure long-term durability, which guarantees the assumed reuse-recycling plan at the end of the projected building's service life.

The deterioration of RC elements is primarily influenced by carbonation and chloride penetration, as defined in the Structural Code

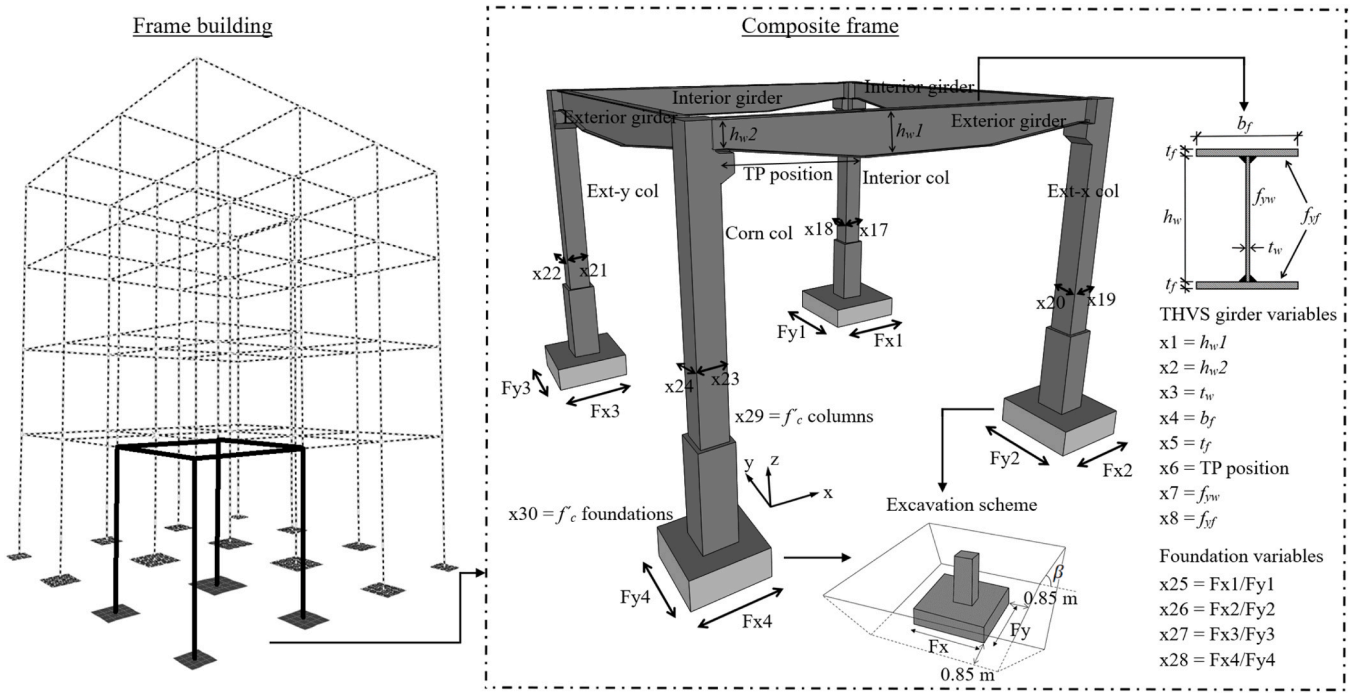

Fig. 3. Visual depiction of the variables defined for the composite design optimization problem.

[45]. The service life (*SL*) of RC elements is evaluated using Tuutti's model (1982) [46] as expressed in Eq. 7. It considers parameters such as concrete cover thickness d (mm), carbonation rate coefficient k (mm/year$^{0.5}$), reinforcement bar diameter ∅ (mm), and corrosion rate v_c (μm/year) [47]. The carbonation rate coefficient varies based on concrete type (see Table 2), while the corrosion rate depends on exposure conditions. Under low-aggressiveness conditions, the corrosion rate is 2 μm/year, whereas under high-aggressiveness conditions, it increases to 20 μm/year. In this study, a standard concrete cover thickness of 30 mm is assumed.

$$SL = \left(\frac{d}{k}\right)^2 + \frac{80 \bullet d}{\varnothing \bullet v_c} \quad (years) \tag{7}$$

When carbonation reaches a critical level, maintenance is required to restore the structural integrity of RC elements. The repair process consists of removing degraded concrete using water blasting, preparing the surface, applying a bonding layer, and using repair mortar to protect reinforcement. In beams, deterioration typically affects the tensioned zone of exposed surfaces, whereas in columns, repairs focus on externally exposed areas. According to BEDEC, maintenance operations for RC elements result in 46.58 kg CO_2 eq emissions per m^2 of repaired surface per maintenance cycle. Each maintenance action occurs at intervals equal to the service life of the RC component. No maintenance for RC elements is required if the calculated building service life exceeds the 100-year projected lifespan.

The amount of CO_2 absorbed through carbonation over the service life is estimated using Eq. 8, based on the diffusion model developed by García-Segura et al. (2014) [47] and the carbonation behavior described by Lagerblad (2005) [48]. The model incorporates factors such as carbonation rate coefficient k, SL duration (years), cement content c (kg/m^3, see Table 2), calcium oxide content in cement CaO (assumed to be 0.65), the proportion of CaO that can be carbonated r (assumed to be 0.75 [48]), the exposed concrete surface area A, and the chemical molar fraction M (CO_2/CaO is 0.79). This approach allows for the long-term evaluation of carbonation's environmental impact in the context of RC durability.

$$CO_2 = k \bullet \sqrt{SL} \bullet c \bullet CaO \bullet r \bullet A \bullet M \quad (kg) \tag{8}$$

For THVS girders, the maintenance strategy follows the guidelines proposed by Helsel et al. (2024) [49] and is based on the international standard ISO 12944:2018 [50], which defines environmental classifications (Part 2) and expected durability ranges for protective coating systems (Part 5). Maintenance is structured into three sequential phases, scheduled according to the coating system's practical service life (P), which depends on the level of environmental aggressiveness. For this study, P is taken as 10 years under low-aggressiveness conditions (e.g., ISO C2) and 5 years under high-aggressiveness conditions (e.g., ISO C5), representing average values for Alkyd-based coating systems as found in the referenced sources.

The first phase, called *spot touch-up and repairs*, is carried out at time P and involves repainting approximately 5 % of the total surface area. The second phase, an *overcoat maintenance repair*, occurs after $1.33\ P$ years, during which the entire surface is recoated with a single layer. The third and final phase is a *full replacement* of the coating system (two coats), scheduled at $P + 0.5\ P$ years, after which the full maintenance cycle restarts. Accordingly, the complete cycle spans 18 years in low-aggressiveness environments and 9 years in high-aggressiveness conditions. The emissions associated with all painting activities in the maintenance phase are assumed to be equivalent to those calculated in the manufacturing stage.

The end-of-life phase includes demolition, disassembly, concrete crushing, and recycling. The demolition of joints generates 6.28 kg CO_2 eq [39]. Steel THVS girders are considered demountable, so energy consumption for their separation is ignored. A crane is used to disassemble the structure, following the specifications for assembling THVS girders. Concrete is crushed on-site, with an associated emission of 0.47 kg CO_2 eq per cubic meter according to Ecoinvent v3.7.1. Structural

Table 2
Coefficients for service life estimation.

Concrete type (MPa)	k (mm/year$^{0.5}$)	c
25	4.41	260
30	3.71	280
35	3.01	300
40	2.50	320

steel recovery rates are estimated at 93 % reusability and 7 % recyclability [51], saving 0.5 kg CO_2 eq per kilogram of recycled steel [52]. In contrast, RC elements exhibit lower reusability at 42 % but are 58 % recyclable [51]. Replacing virgin aggregates with recycled concrete aggregates results in a 40–60 % reduction in emissions, estimated at 40 kg CO_2 eq per cubic meter of recycled concrete [53]. The recycling impact of reinforcing steel is calculated similarly to that of structural steel.

2.2.2. Design variables

This research addresses two types of optimization problems, both defined using discrete variables. The first problem corresponds to a conventional structural typology, aligning with the methodology adopted in previous research [7]. It involves 19 design variables, with the initial four governing the dimensions of RC beams. These beams are divided into two categories: interior and exterior. Beam depth is determined based on the span length L, which can assume 11 discrete values. The minimum allowable depth is calculated as $L/18$, rounded to the nearest 5 cm increment, while the upper limit is set to accommodate all 11 predefined depth options. For instance, when $L = 4$ m, the resulting depth values shift from 0.25 m to 0.75 m. Beam width is also discretized, with five possible values. For spans of 4 m or 6 m, the minimum width is 0.20 m, whereas for spans of 8 m, the minimum increases to 0.25 m to ensure structural adequacy.

Eight additional variables define the columns' dimensions, which are grouped within four categories: interior, exterior along the x-axis, exterior along the y-axis, and corner columns. These dimensions are restricted to multiples of 5 cm, with values ranging from 0.25 m to 0.60 m, resulting in eight discrete options.

Another four variables control rectangularity of the foundation groups (*Fx/Fy*, see Fig. 3), following the same four column groupings. Each foundation group can adopt one of nine predefined discrete values: 0.50, 0.63, 0.75, 0.88, 1.00, 1.25, 1.50, 1.75, or 2.00.

The remaining three variables determine the type of concrete used for beams, columns, and foundations. Fig. 3 presents an overview of the geometric variables associated with columns and foundations, as well as the concrete type assignments.

In the composite typology, RC beams are replaced with THVS girders, increasing design complexity. While the traditional model includes four beam-related variables, the composite system introduces 16 variables, eight for each girder group (interior and exterior). It is important to note that the formulation of these elements, including the method for assessing their environmental impact, the definition of design variables and their intervals, and the imposed design constraints, is based on previous studies developed in collaboration with experts from the steel manufacturing industry [21,22], ensuring practical applicability.

The first two variables (*x1*, *x2*) define the central and end section heights (h_w1, h_w2), each selectable from 31 values in 10 mm increments (e.g., *x1* = [100, 110, …, 400] mm). These intervals vary by girder group and case study. For example, in the $L = 8$ m span case (CS-3) with pinned joints (Fig. 3), h_w1 for interior girders ranges from 700 to 1000 mm, while the outer section remains between 100 and 400 mm. These bounds are based on prior studies, and intervals are adjusted if optimal values consistently cluster at extremes, ensuring a more centered and efficient search range.

The third variable (*x3*) controls the web thickness (t_w), with four discrete values: 5, 6, 8, and 10 mm. The fourth (*x4*) and fifth (*x5*) variables define the flange width (b_f) and flange thickness (t_f), respectively. The flange width can take 11 discrete values in 10 mm increments, starting from 100 mm. The flange thickness follows the same set of values as t_w, except when $L = 8$ m, in which case the options are limited to 6, 8, 10, and 12 mm.

The transition point (TP), marking the change in geometry between variable and constant sections in the variable-section element (*x6*, see Fig. 3), is defined at discrete 50 mm intervals to facilitate constructability. For $L = 4$ m cases (CS-1 and 2), this variable has 39 possible values, increasing to 79 in the $L = 8$ m case (CS-3). The final two variables (*x7*, *x8*) define the web's (f_{yw}) and flanges' (f_{yf}) steel quality, with eight available steel grades: S235, S275, S355, S420, S450, S500, S550, and S600.

Subsequently, in the composite typology, the five variables originally associated with RC beams (four related to geometry and one to material) are replaced by 16 new variables that define THVS girders' design. This modification increases the total number of discrete variables to 30, as shown in Fig. 3.

2.2.3. Constraints

The optimization problem includes two types of constraints. Design (explicit) constraints define allowable ranges for variables, based on constructability, architectural, and functional considerations, such as the movement intervals described earlier. Behavioral (implicit) constraints, or state equations, ensure compliance with structural performance criteria by enforcing limit states derived from design codes and standards. These are typically formulated as in Eq. 9.

$$g_j(x1, x2, \ldots, xn) \leq 0 \tag{9}$$

For RC frame elements, ultimate limit state constraints are inherently satisfied via the SAP2000-MATLAB API, which calculates the required reinforcement area per design standards and converts it into practical bar configurations. Foundation design, covering both geotechnical and structural aspects, is handled through a custom MATLAB routine.

THVS girder constraints are evaluated using a MATLAB-based procedure aligned with the methodology in [22], assessing bending capacity, shear strength, lateral-torsional and shear buckling, flange-web buckling, and stiffness. Unlike RC elements, THVS design uses a verification-based approach: a configuration is proposed and checked for compliance. If it fails, a penalty is applied to the objective function, discouraging infeasible solutions. This penalty mechanism also enforces serviceability constraints, such as RC cracking, reinforcement spacing, lateral drift, and girder stiffness. Penalty values are scaled to the severity of violations, guiding the optimizer toward feasible, high-performance solutions.

2.3. Solution of the LCEIO problem

A key challenge in these optimization problems is the high computational cost of HFS, which require substantial resources for each finite element analysis. When exploring large design spaces, performing thousands of such evaluations using traditional optimization methods becomes impractical.

To overcome this, a more efficient alternative is proposed. The method reduces computation time while preserving optimization quality by initiating the process with a design of experiments strategy. Latin Hypercube Sampling (LHS) generates a well-distributed set of N initial solutions, minimizing redundancy. A local search then refines results by starting from the best-performing candidate in the initial set. This approach raises the dilemma of whether to set a low value of N to save valuable HFS at the cost of reduced diversity in the initial population, or to enhance this diversity by increasing the computational cost of the process. For the problems addressed in this study, trial-and-error testing determined that $N = 100$ yields stable results.

2.3.1. The CINS algorithm

The Constrained Iterative Neighborhood Sampling (CINS) algorithm, proposed by Negrin et al. (2023a) [7], is implemented to perform the local search phase. This algorithm is specifically designed for discrete optimization problems, particularly when the number of possible values for each variable is not excessively large. A key advantage of CINS is that it does not require parameter tuning, offering standardized behavior that can be directly applied to a wide range of discrete optimization problems without algorithm-specific calibration. An improved version

of CINS is developed for this study, as outlined in the diagram in Fig. 4 (a).

The algorithm operates by performing unit steps in both directions (±1) for each variable of the current solution, a process referred to in the diagram as "updating the current state". This basic solution starts the iteration. In each iteration's first step, the algorithm requires at most twice the number of design variables to evaluate new solutions through HFS. However, suppose a variable is already at its upper or lower limit. In that case, only a single unit step is performed in the allowable direction, thereby reducing the initial number of required HFS. The objective function values corresponding to these unit steps are stored.

Once this initial phase is completed, the algorithm analyzes the results and identifies the set of "n" solutions that improve upon the basic one. If no improvements are found ($n = 0$), the process terminates, and

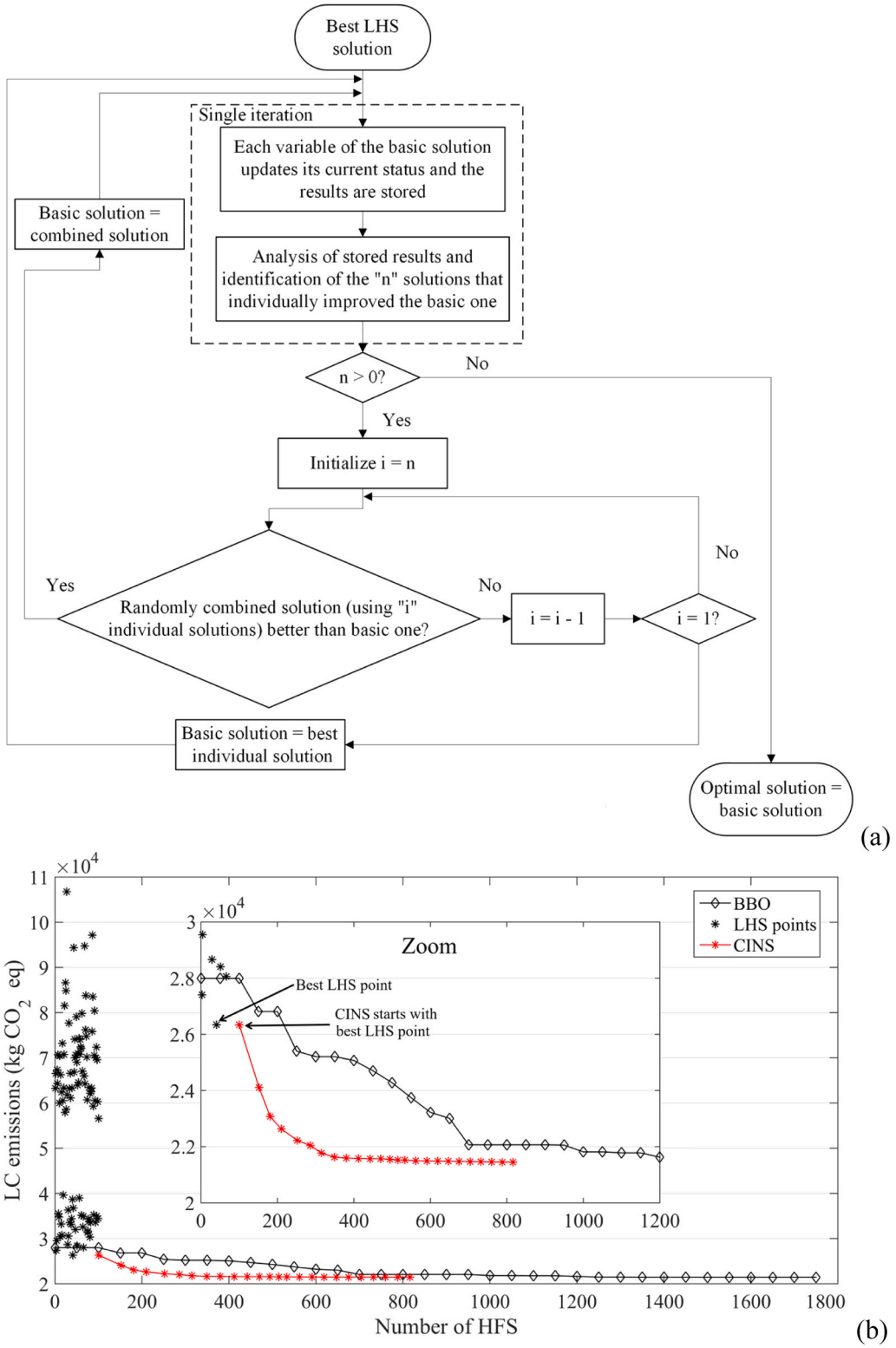

Fig. 4. (a) Flowchart of the CINS algorithm; (b) comparison of the LHS-CINS methodology performance with the BBO heuristic.

the current basic solution is considered the local optimum. Otherwise, the improving solutions are combined in a structured, descending order. If $n = 5$, for instance, the five best solutions are first combined to form a new candidate solution. While this initial combination is not random since all available improvements are incorporated, subsequent combinations are randomly formed.

If the combined solution improves upon the basic one, it becomes the new basic solution, and a new iteration begins. If not, the process continues by combining only four of the best solutions, then three, and so forth. If none of these combinations yield an improvement, the best individual solution among the original "n" candidates is selected as the new basic solution and a new iteration starts.

All tested solutions and their corresponding objective function values are stored in a database to enhance efficiency. This prevents redundant HFS evaluations for solutions that have already been analyzed. It is important to note that, although CINS is classified as a “local search” method, its design allows it to escape local optima by enabling the combination of up to n solutions multiple times within the same iteration. For further details on the algorithm’s underlying principles, refer to [7].

The graph on Fig. 4(b) compares the performance of a traditional heuristic algorithm, Biogeography-Based Optimization (BBO), with the proposed LHS-CINS strategy. Originally introduced by Simon (2008) [54], BBO is widely recognized for its rapid convergence and effectiveness in solving discrete structural optimization problems [7].

The case presented corresponds to the composite typology with rigid joints in case study 1, set in a low-aggressive environment. The results show that the hybrid LHS-CINS strategy converges significantly faster than BBO, achieving an outstanding solution of 21,452 kg CO_2 eq while requiring 53 % fewer HFS. The BBO parameters were tuned to maximize performance, ensuring a fair comparison. Overall, the proposed strategy delivers high-quality solutions in about half the time of a conventional heuristic. Notably, it outperforms BBO, a method the authors have been improving for discrete structural optimization over the years, while maintaining computational feasibility and solution reliability, underscoring LHS-CINS as a robust and time-efficient alternative.

Due to the stochastic nature of the initial sampling, each case is evaluated through three independent runs, with the best-performing solution selected. If significant discrepancies arise, additional runs are conducted until consistent results are achieved. Importantly, the goal of heuristic optimization in structural applications is not to find a theoretical global optimum but to deliver competitive solutions within reasonable computational limits. In this context, LHS-CINS maintains high accuracy while significantly reducing computational demands, improving the scalability and practicality of life-cycle-focused optimization for complex structural systems.

3. Results and discussion

The analysis begins by comparing the life-cycle performance of optimized structural solutions against traditional design approaches, focusing on reductions in environmental impact. This is followed by evaluating the environmental performance of the two composite typologies in relation to the conventional RC system. Based on the results of the life-cycle optimization, a parametric analysis is then carried out to systematically investigate how variations in key design parameters affect the performance of the composite systems. This step aims to identify configurations that further enhance sustainability and structural efficiency. The analysis extends to assess the robustness of the optimized configurations when applied to buildings with stiffer superstructures, incorporating the effects of slabs and structural walls. Finally, the most important results and limitations are discussed, thereby laying the groundwork for future research.

3.1. Influence of LCEIO

The importance of structural optimization is illustrated through a comparison with a conventional RC design applied to case study CS-1 under two environmental aggressiveness levels. In the traditional design, all beams use a uniform 0.50 × 0.20 m cross-section, matching the optimized interior beam size, while columns follow standardized square sections: 0.45 m for interior and 0.35 m for exterior and corner locations. The foundation consists of square footings, with all elements cast in 30 MPa concrete.

In contrast, the composite typology retains most RC elements, except for reduced interior columns (0.40 × 0.40 m), and replaces RC beams with S355-grade W steel profiles selected from a predefined list based on structural efficiency and weight minimization. Interior and exterior elements are differentiated as in the optimized scheme.

As shown in Fig. 5, life-cycle optimization outperforms the conventional approach, reducing impact by ~15 % in RC designs and over 30 % in composite systems, particularly with fixed joints. At the element level, the best-performing composite configuration (Comp F) shows a 47 % reduction in THVS girder impact under both exposure conditions, exceeding 50 % in low-aggressiveness environments. Additionally, column and foundation impacts are reduced by 24 % and 13 %, respectively.

THVS girders with pinned joints (Comp P) achieve a notable 55 % reduction in environmental impact compared to traditional profiles, marking them as the most individually improved elements. However, this typology performs worse globally than its fixed-joint counterpart due to reduced stiffness, which shifts demand onto the columns, significantly increasing their environmental impact. While columns and foundations still perform better than in the conventional design, their indicators remain weaker relative to other optimized typologies.

Fig. 6 details the life-cycle evolution of the solutions from Fig. 5. THVS girders show major advantages in the manufacturing stage due to superior material efficiency, with fixed-joint configurations yielding 65 % lower emissions than I-profiles, and pinned joints achieving up to 74 % reduction. Both systems have minimal impact in the construction phase, thanks to ease of installation. During maintenance, optimized typologies reduce emissions by ~45 %, largely due to THVS’s tapered geometry, which enhances material distribution. However, this advantage narrows at the end-of-life stage, where traditional profiles offer more potential for reuse and recycling due to their higher material mass.

A similar situation occurs with the columns since design optimization significantly reduces manufacturing impacts. For example, by optimizing the fixed composite typology, the emissions of producing the formwork, steel, and concrete to build the RC columns are reduced by 27 % compared to the traditionally designed structure.

3.2. Advantages of the composite typology

In the previous section, the advantages of the composite typology over the traditional RC typology (particularly in the rigid connection configuration) were preliminarily demonstrated. This chapter provides a comparative analysis of the three optimized typologies using the three case studies. The results are categorized based on the two distinct environmental conditions in which the structures are situated.

3.2.1. Low aggressiveness

Fig. 7 presents net emissions for each optimized typology across three case studies in low-aggressive environments. As expected, the composite system with rigid beam-column connections outperforms both alternatives. THVS girders consistently demonstrate superior environmental performance compared to traditional RC beams. In CS-1 and CS-2 (4 m span girders), emissions are reduced by ~56 % and by 44 % in CS-3.

Beyond girders, the rigid composite typology also reduces the impact of columns and foundations. Column emissions are lowered by 16.31 %,

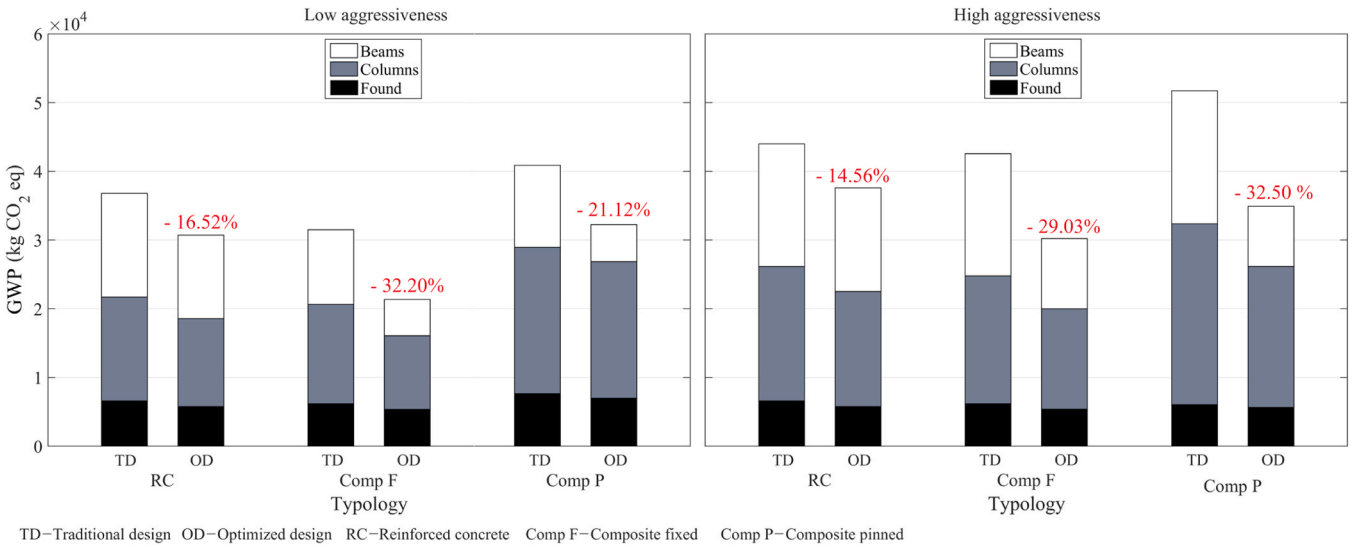

Fig. 5. Comparison broken down into elements between traditional and optimized design for each typology using the CS-1.

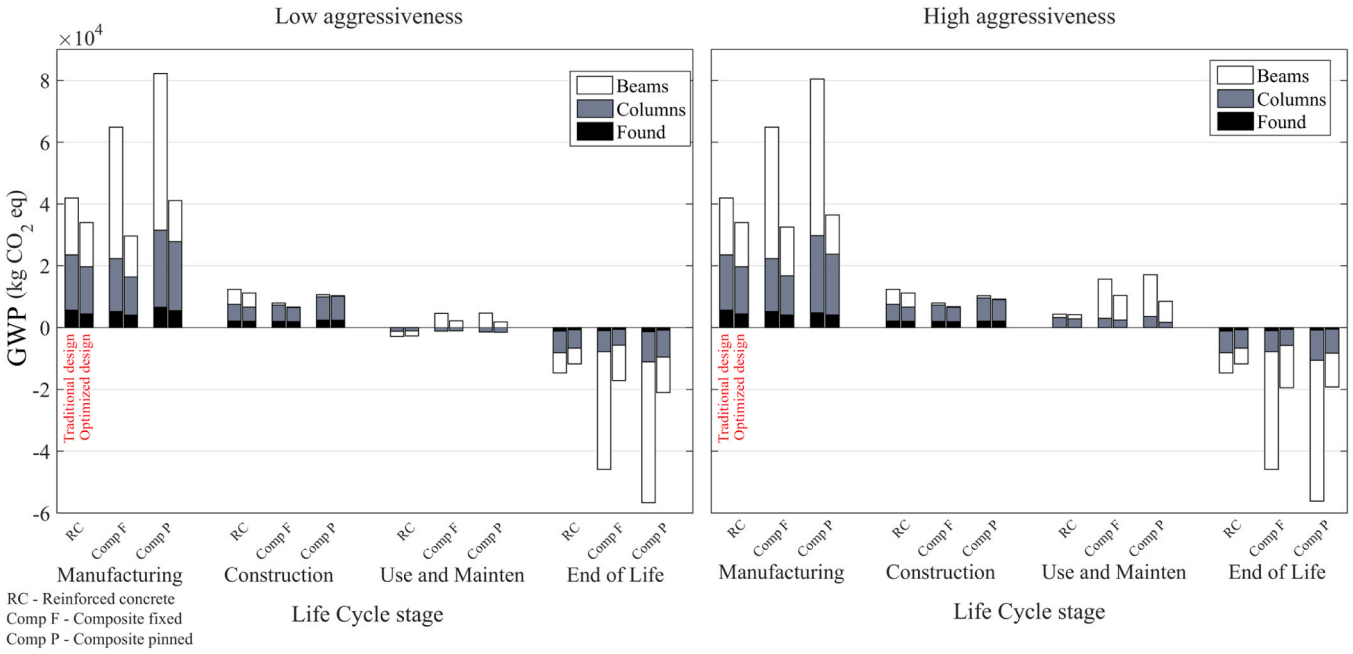

Fig. 6. Impact of each life cycle stage broken down into elements for both types of exposure. For each typology, two sets of bars are shown: the one on the left is the traditional design, while the one on the right is the optimized one.

14.37 %, and 8.42 % in CS-1, CS-2, and CS-3, respectively. Foundation emissions decrease by 6.90 %, 6.70 %, and 12.12 %. These reductions stem from the decreased structural weight enabled by THVS girders, as other variable configurations remain unchanged across typologies.

As previously stated, the reduced stiffness of the composite typology with pinned beam-column connections adversely affects the design of load-bearing elements. Consequently, despite the strong individual performance of pinned THVS girders, the overall structural system exhibits a significantly higher environmental impact.

Fig. 8 highlights a nuanced result: in CS-2 and CS-3, THVS girder production generates slightly higher emissions than traditional RC beams due to additional manufacturing steps like plate cutting and welding. However, their advantages (lower construction-phase impact and superior dismantling potential due to ease of disassembly and high reuse/recycling rates) offset this. Their optimized geometry and reduced weight improve overall life-cycle efficiency. While RC beams may exhibit a marginally lower initial footprint and benefit from CO_2 uptake in later stages, THVS girders achieve significantly lower total impact.

The manufacturing phase dominates total emissions, while the "use and maintenance" stage contributes minimally. It is because optimized RC elements surpass a 100-year service life with no required maintenance under low-aggressiveness conditions and appropriate concrete cover. Only the THVS girders undergo preventive maintenance, which supports reuse without significantly impacting emissions.

3.2.2. *High aggressiveness*

In aggressive environments, Fig. 9 shows that the composite typology, while still outperforming the traditional system, loses some of its relative advantage, particularly in the fixed-joint configuration. Interestingly, the pinned-joint variant improves its performance relative to the conventional system under these harsher conditions. On average, the fixed-joint composite system achieves a 21 % reduction in impact

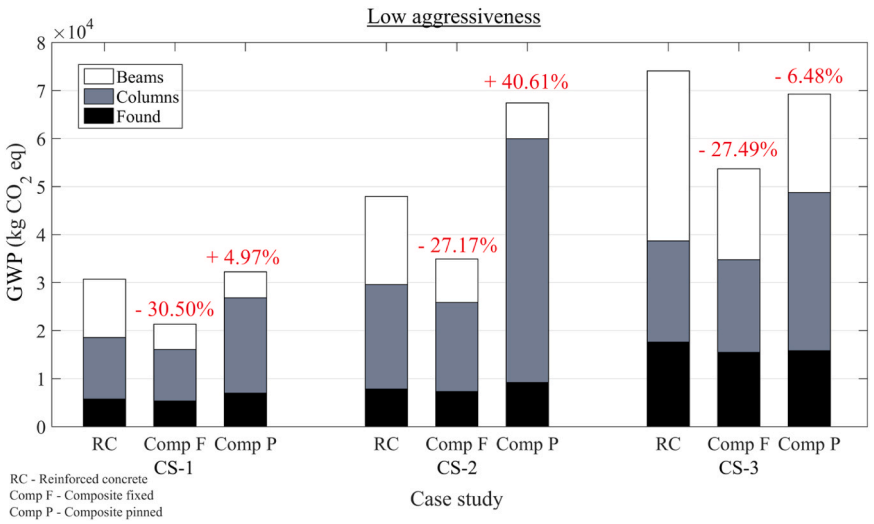

Fig. 7. Life cycle impact of the three typologies optimized in the three case studies for low-aggressive environment.

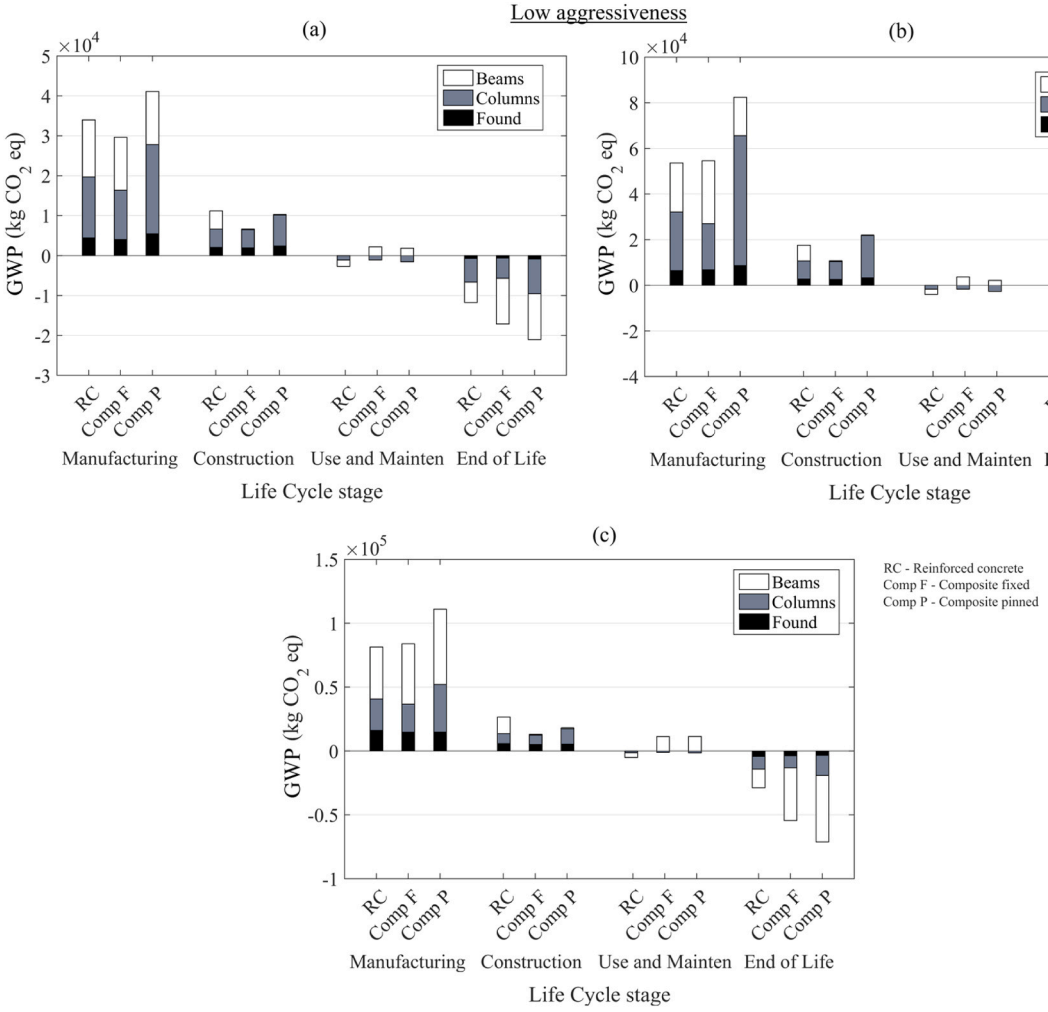

Fig. 8. Impact of each life cycle stage broken down into elements of the three typologies evaluated in case studies (a) 1, (b) 2, and (c) 3 for low aggressiveness.

compared to the traditional system, down from 28 % in low-aggressiveness environments. In contrast, its performance gap narrows in CS-2, where it is only 7 % less efficient, compared to a 13 % disadvantage under less aggressive conditions.

This decline in effectiveness is primarily due to the increased impact of the third stage (maintenance) highlighted in Fig. 10. While other life-cycle stages remain relatively stable, maintenance-related emissions for steel elements rise sharply in more aggressive environments. In

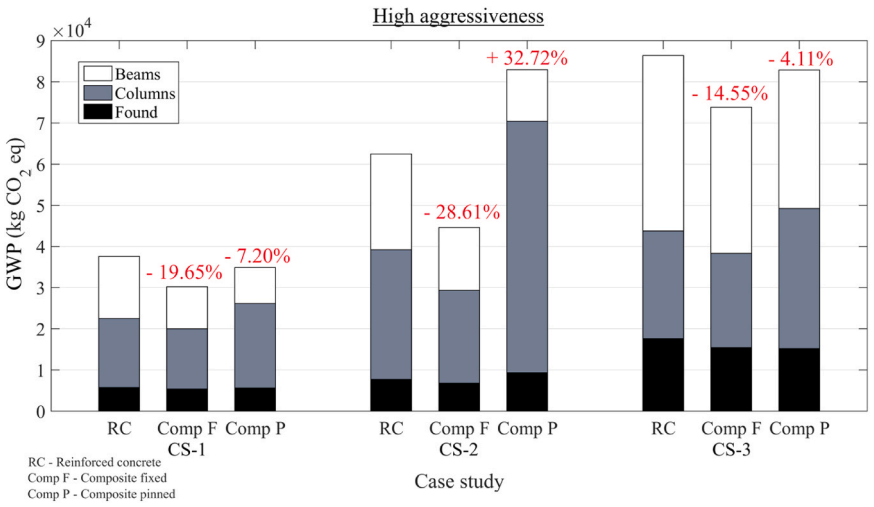

Fig. 9. Life cycle impact of the three typologies optimized in the three case studies for high-aggressive environment.

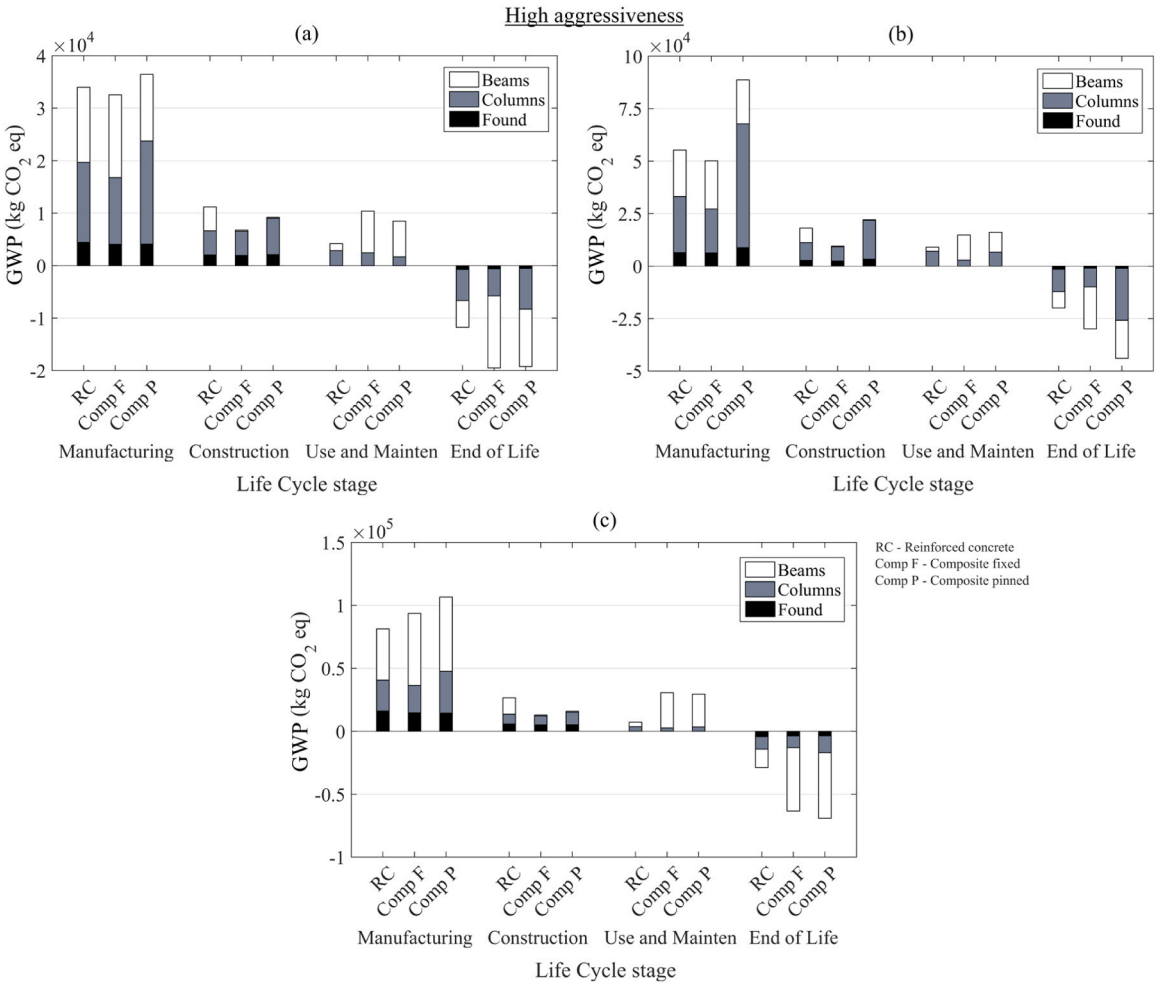

Fig. 10. Impact of each life cycle stage broken down into elements of the three typologies evaluated in case studies (a) 1, (b) 2, and (c) 3 for high aggressiveness.

traditional systems, the third-stage impact increases from negligible to over 12 % of the manufacturing stage's impact. For the composite typology, it jumps from 7 % to 28 %, significantly affecting its overall environmental performance.

Even with this increase in emissions in the third LCA stage for more hostile environmental conditions, its impact on frame-type buildings does not seem as significant as it could be in other structures, such as load-bearing wall buildings or bridges. This may be due to the surface area being exposed to deterioration, which is much higher in this second group of structures.

Although the fixed-joint THVS typology loses some relative advantage in high-aggressiveness environments, the core benefits observed

under low-aggressiveness conditions remain consistent. As shown in Fig. 11, this system not only improves its own environmental performance relative to conventional RC beams but also enhances overall structural efficiency due to reduced self-weight. Notably, exterior columns in the composite structure experience 17 % lower axial forces than those in the traditional system under the load combination of Eq. 1, reducing also demands on the foundations.

3.3. Parametric study of optimal composite designs

With the superiority of the composite typology established, this section examines the key parameters influencing its optimal configurations.

3.3.1. THVS girders

Regarding the geometry of the THVS girders, the key parameters analyzed include the span-to-depth ratio (L/d) for both cross-sections, and the transition point where the element shifts from a conical to a prismatic shape. In terms of material configuration, the study focuses on the selected steel grades for the flanges and web, with the corresponding hybrid ratio R_h. Fig. 12 exhibits 3D representations of the optimal solutions obtained for the CS-1 in a low-aggressive environment, illustrating the analyzed parameters.

Fig. 13 illustrates the relative position of the transition (used to group girders with different spans) as a function of the L/d ratio. This representation provides insight into the overall behavior of the tapered distribution under varying conditions. For instance, the figure enables the establishment of pre-dimensioning criteria based on environmental aggressiveness while also facilitating comparisons between different configurations for each case.

Interestingly, fixed configurations, particularly exterior ones, exhibit larger web surface areas in high-aggressiveness environments. While this might appear counterproductive due to increased maintenance impact, it is likely influenced by structural interdependencies. For example, deeper sections can reduce flange material, potentially lowering the flange surface area needing maintenance. Conversely, smaller web areas may extend the lower flange length, increasing its surface area.

These stiffer configurations can also reduce the stiffening demands on the columns, leading to smaller concrete sections. As shown in Fig. 10 (b), column maintenance impact is significantly lower for these solutions. It is important to note that Fig. 13 displays averaged values across all case studies. Overall, these trends suggest that the maintenance phase (Stage 3) does not dominate the total life-cycle impact for this building type.

In pinned configurations, tapered girders behave consistently across aggressiveness levels. Like their fixed counterparts, interior girders tend toward a more prismatic shape, consistent alignment observed in key geometric parameters, particularly the transition placement.

Regarding material configuration, Fig. 14 reveals a clear preference for hybrid configurations, with only two cases retaining a homogeneous design. However, the current R_h values are lower than in previous studies, where only the manufacturing process impact was optimized.

A notable trend is the frequent use of high hybrid ratios in exterior girders (indicated by red symbols), primarily due to the widespread use of lower-grade steel (S235) for their webs. In fact, 75 % of exterior girders, regardless of joint type, utilize S235 webs, reinforcing this pattern across configurations.

The most efficient material combinations vary by environment and connection type. In low-aggressiveness settings, fixed-joint interior girders use S420 webs and S500 flanges, while exterior girders adopt S235-S420. In pinned-joint configurations, the optimal pairing is S235-S420 for interior girders and S235-S275 for exterior ones.

In high-aggressiveness environments, fixed-joint interiors use S355-S500 and exteriors S235-S355. For pinned-joint girders, both interior and exterior elements rely on S235 for webs and S355 for flanges. These patterns reflect the lower structural demands and greater material efficiency achieved with lower-strength steels in pinned configurations compared to their fixed counterparts.

3.3.2. Columns and foundations

For columns and foundations, the analysis focuses on cross-section rectangularity for columns and base dimensions for footings. Fig. 15 shows the rectangularity trends across the four groups of columns. A key observation is the data's symmetry about the red line (representing square sections), indicating a balanced stiffness distribution in both horizontal directions. It is consistent with the symmetrical floor plans in all case studies, which experience uniform lateral loading.

Additionally, in both environmental conditions, a clear pattern emerges: "x" markers (interior columns) lie mostly below the red line,

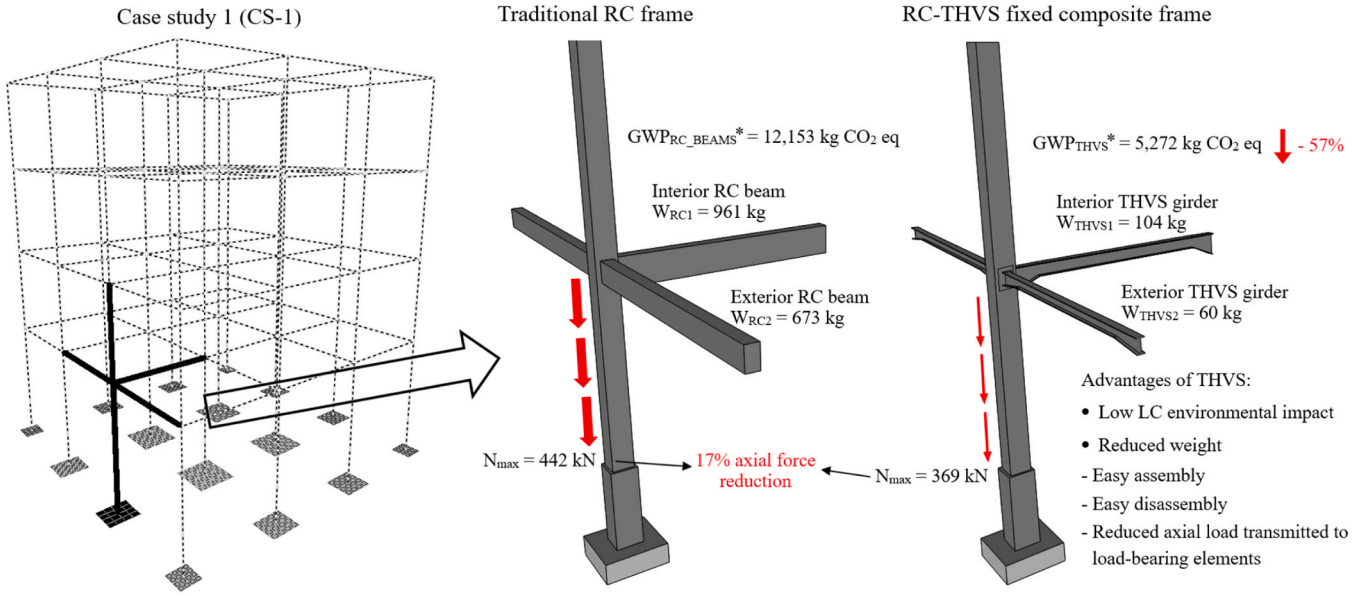

Fig. 11. Representation of some advantages of THVS girders over their traditional counterparts. Both variants depicted are evaluated in the base case study for a low-aggressive environment. *GWP indicators pertain to all beam-type elements of each building system.

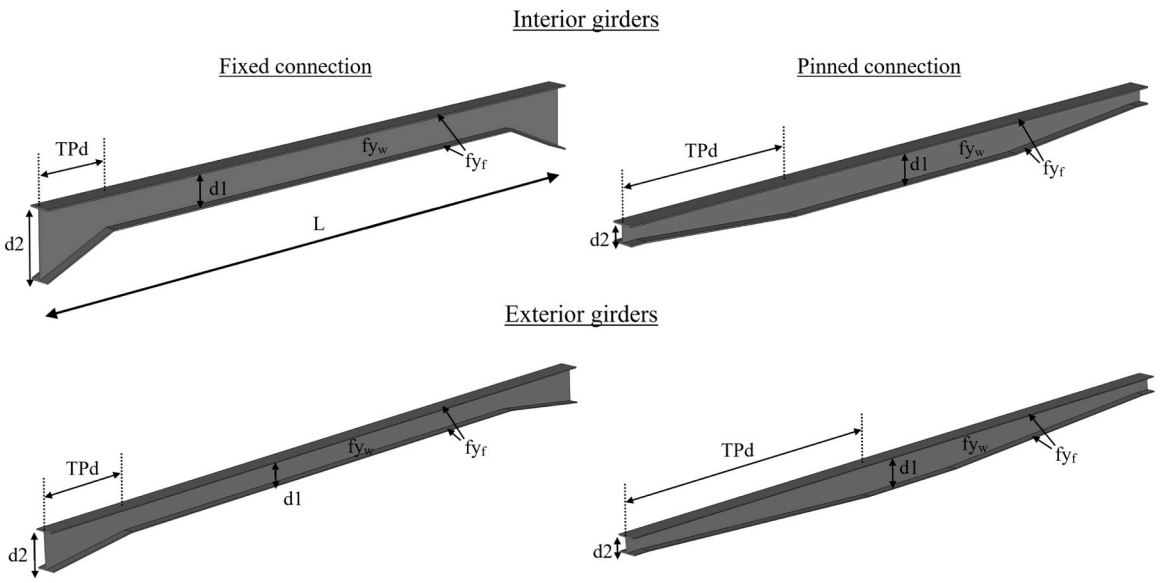

Fig. 12. 3D representation of the optimal THVS configurations obtained for the CS-1 for low aggressiveness.

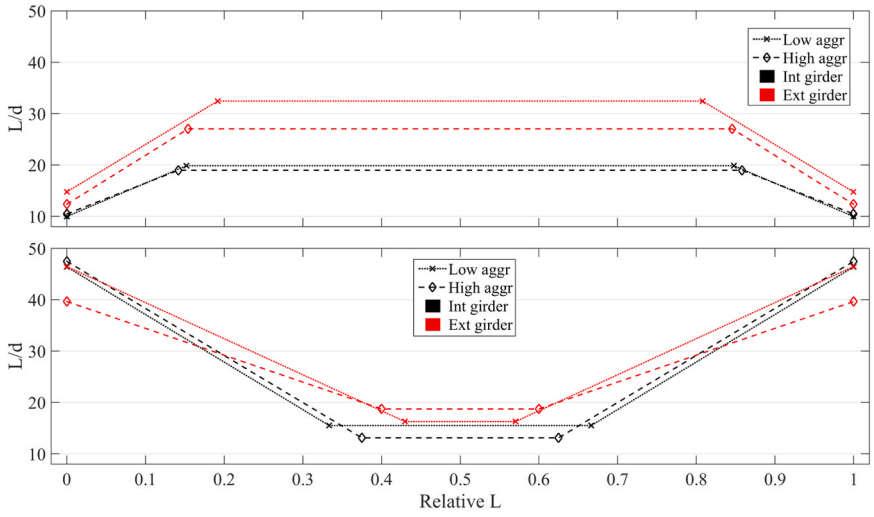

Fig. 13. *L/d* ratio as a function of the (relative) position of the transition point. Top: Fixed configurations. Bottom: Pinned configurations.

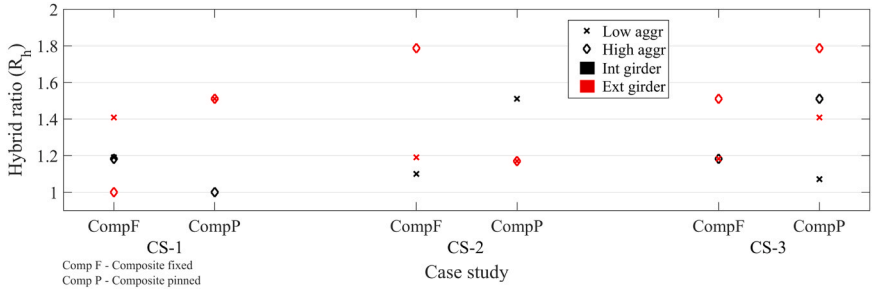

Fig. 14. Optimal R_h values of both THVS typologies for the three case studies.

while diamonds (◊, exterior columns) tend to be above. It suggests that exterior columns are designed with larger cross-sectional dimensions perpendicular to their main axis, enhancing stiffness to resist gravity-induced bending better.

In exterior columns aligned along the x-axis, bending from gravity loads primarily occurs in the y-direction. This is because beams connect from both sides in the x-direction, canceling eccentricity effects, while in the y-direction, connections are typically one-sided, inducing moment. The reverse applies to y-axis columns.

Consequently, columns are optimally designed with rectangularity oriented opposite to their primary bending axis, enhancing resistance to gravity-induced moments and contributing to balanced horizontal

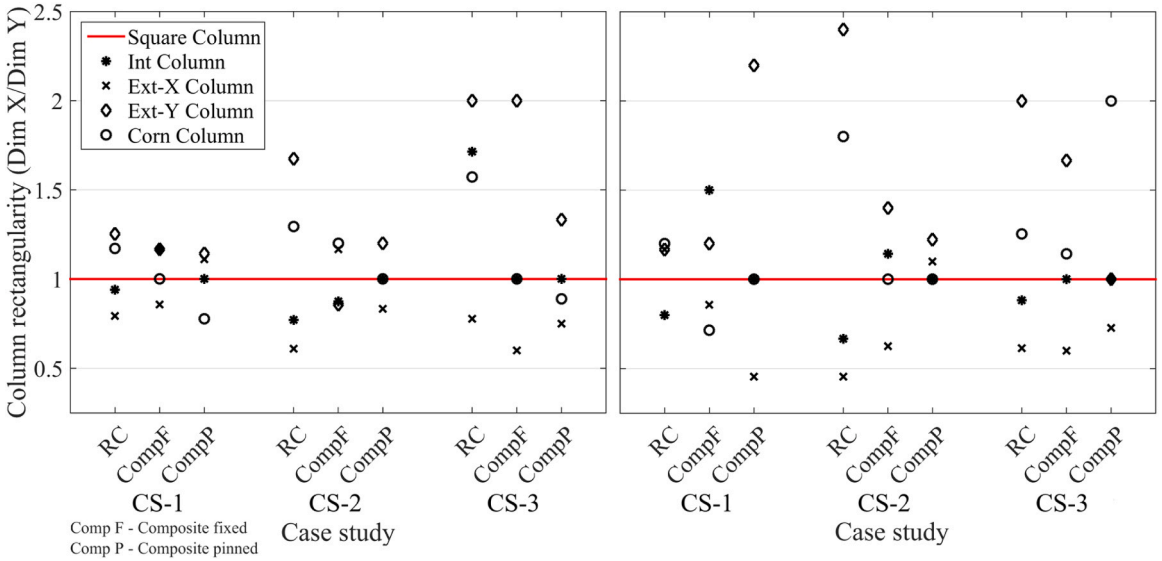

Fig. 15. Optimal rectangularity of each column group for each typology based on the case study, shown for the two environmental conditions: Left – low aggressiveness, Right – high aggressiveness.

stiffness across the structure.

In highly aggressive environments, increased rectangularity, especially in exterior columns, suggests a strategy to expand cross-sections inward. This improves structural performance and reduces the area exposed to harsh conditions, thereby lowering maintenance demands.

The optimal solutions for concrete quality in columns favor high-strength concrete (35–40 MPa). This choice addresses two key objectives. First, it ensures sufficient durability to avoid maintenance under low-aggressiveness conditions and reduces the required maintenance cycles in highly aggressive environments. Second, it significantly enhances the load-bearing capacity of these elements, which primarily work in compression.

Regarding the foundations, Fig. 16 reveals a consistent trend of low rectangularity across all foundation groups. Notably, among all cases, only one point (red diamond in the *CompP* typology for the CS-1) deviates significantly, positioned three steps away from the square foundation value. Additionally, very few points fall one or two steps from the square solution, and none are placed at the extremes (four steps away). Most points align with the red line, indicating zero rectangularity, meaning most footings maintain a square shape.

However, similar trends can be observed in comparison to the columns. Notably, most "x" markers appear below (or on) the red line, while only a few are above. In contrast, diamond markers are more frequently positioned above or directly on the line rather than below. This pattern suggests that foundations predominantly feature square bases or slightly rectangular ones. Exterior foundation groups, in particular, can follow a low-rectangularity pattern to withstand better the bending induced by gravity loads in the same direction as the associated columns.

In contrast to columns, optimal solutions use the least environmentally impactful concrete (25 MPa) for the foundations. It is because foundations in the proposed system are primarily subjected to flexural demands and are not evaluated in terms of durability, as they are not exposed to carbonation. As a result, using higher-grade concrete, which carries a greater environmental burden, would only increase the overall impact without providing meaningful structural or durability benefits.

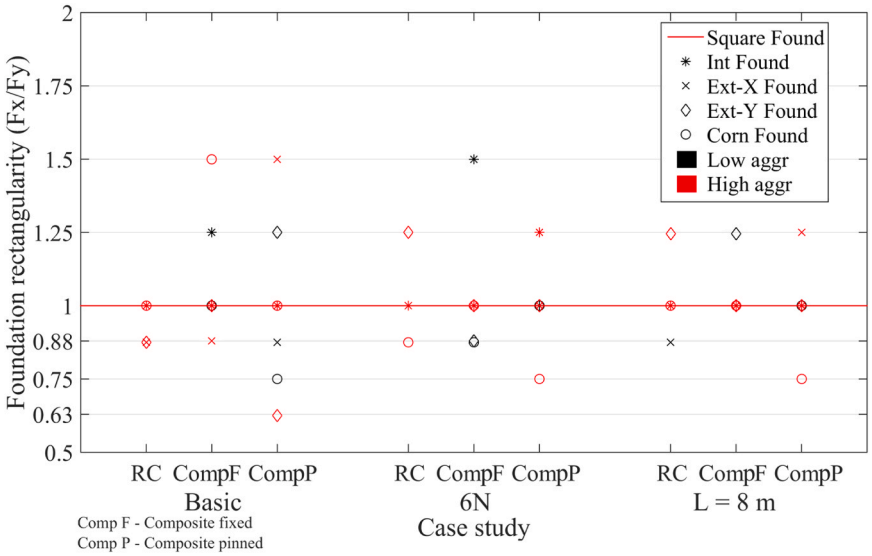

Fig. 16. Rectangularity of foundation groups of the three typologies in the three case studies located in both types of environments.

3.4. Influence of additional stiffening elements

As previously discussed, a main limitation of the THVS typology, particularly the pinned-joint variant, is its lower stiffness compared to RC frames. While pinned THVS girders perform best individually among beam elements, their low stiffness forces columns to compensate, increasing overall environmental impact.

This analysis considers buildings where beams simply support slabs and walls have no structural role, requiring the frame alone to resist lateral loads. Even under these conditions, the RC-THVS system with fixed joints outperforms the conventional RC design. This prompts an important question: how would performance change if slabs and walls contributed to global stiffness?

To explore this, cases 2 and 3 are re-optimized under low-aggressiveness conditions by incorporating slabs and walls into the structural model. Using the methodology from Negrin et al. (2025a) [12] and illustrated in Fig. 17, slabs are modeled as 12 cm-thick solid shell elements, fixed to beams to ensure vertical co-deformation. Infill masonry walls are represented by equivalent diagonal struts acting only in compression. For modeling details, refer to [12].

Fig. 18 confirms that incorporating stiffening elements significantly improves the environmental performance of composite typologies, especially the pinned-joint configuration. In CS-2, system-wide impact drops by nearly 42 %, with columns alone showing a 46 % reduction. The added stiffness also benefits THVS girders and foundations, enhancing overall efficiency.

Despite these gains, the rigid-joint typology remains the most effective for buildings with small spans, achieving a 7.80 % overall impact reduction, with girders seeing the most significant improvement.

In contrast, for large-span buildings where slabs and walls contribute structurally, the pinned-joint configuration becomes the optimal solution, reducing life-cycle impact by over 30 %, including a 54 % reduction in column impact. Meanwhile, the rigid-joint alternative offers only a modest 3.58 % decrease, underscoring the superior adaptability of the articulated system under these conditions.

3.5. Discussion and future perspectives

The findings of this study highlight the significant environmental benefits that can be achieved through structural optimization, particularly when composite typologies are employed. One of the clearest trends is the optimization algorithm's effectiveness in minimizing environmental impact during the early life-cycle stages, especially manufacturing. At the same time, the algorithm is able to address key trade-offs that arise in these phases, for instance, recognizing that the lowest initial-cost solutions are not always the most durable, and may therefore incur greater maintenance-related impacts during the use stage. It reinforces the superiority of integrating artificial intelligence algorithms as design tools over traditional approaches that rely solely on the designer's experience. In this study, optimizing environmental impact across the entire life cycle makes it possible to achieve a global reduction of more than 30 % compared to traditionally designed or non-optimized solutions.

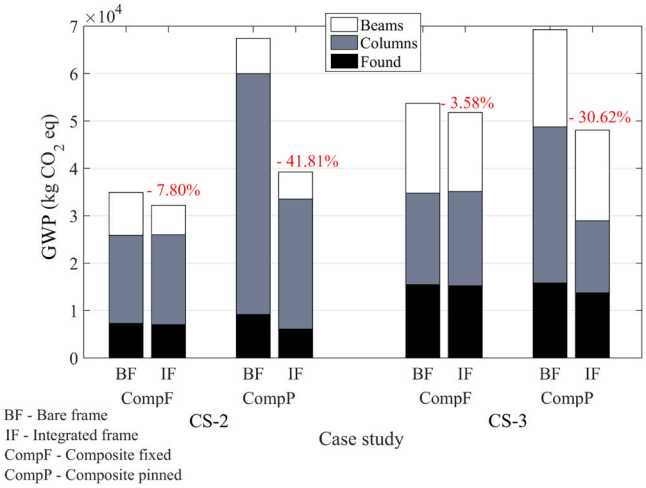

Fig. 18. Environmental impact assessment of the optimized composite typologies for both types of superstructures shown in Fig. 17.

When comparing composite typologies with conventional RC systems (both optimized), the fixed-joint THVS configuration consistently demonstrates superior performance under low-aggressiveness environmental conditions. The reduction in structural weight achieved through optimized THVS girders not only improves their own environmental metrics but also significantly reduces the impact of load-bearing elements such as columns and foundations. This system-wide benefit confirms the cascading effects of targeted optimization at the component level in the form of optimization variables, while capturing their impact on the structural whole.

Nonetheless, the performance of pinned-joint configurations, although promising in terms of solely beam-type efficiency, is limited by their lower global stiffness, which negatively affects the design of the other load-bearing elements. This limitation is especially evident in models where structural slabs and walls are not integrated as an active part of the superstructure.

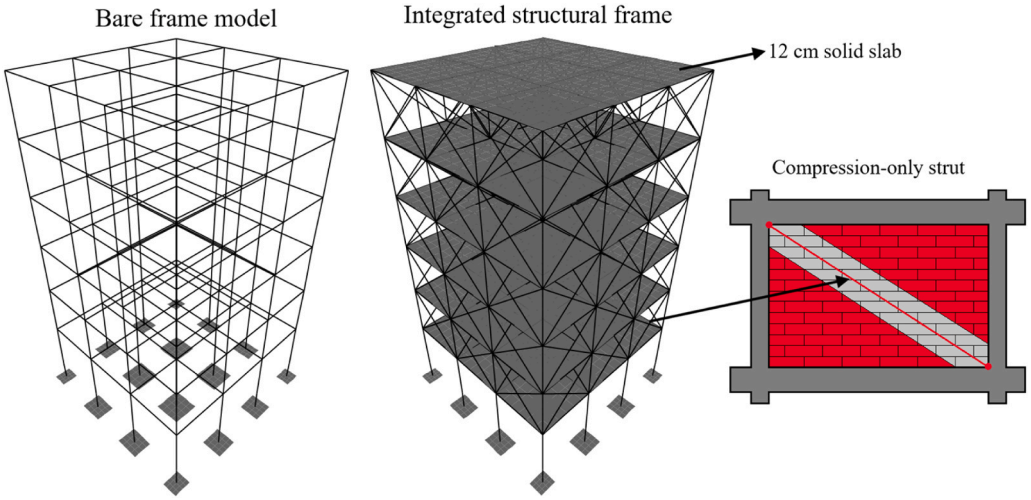

Fig. 17. Inclusion of slabs and infill walls in the superstructure modeling [12].

The parametric analysis of THVS girders further illustrates how granting the optimization algorithm full freedom results in highly efficient, tapered geometries and hybrid material configurations. Notably, when maintenance is factored into the objective function, the algorithm shifts toward less slender designs with reduced steel surface area, producing more balanced solutions that maintain both structural and environmental effectiveness over time. This shift is reflected in the reduction of the R_h values compared to previous studies. It suggests that the web plate is now being designed using higher-quality steel, allowing for minimized material usage while simultaneously reducing the surface area exposed to degradation throughout the structure's life cycle. This distinction highlights the added value of life-cycle-based optimization over early-stage design approaches, emphasizing how material selection influences not just manufacturing but long-term performance and maintenance demands. Altogether, this adaptive behavior underscores hybrid configurations' superior flexibility and structural efficiency compared to homogeneous alternatives.

Finally, including additional stiffening elements, such as slabs and structural walls, profoundly improves the performance of composite typologies, especially for pinned-joint configurations. In scenarios where these additional elements contribute to global stiffness, the limitations of composite configurations associated with lower frame stiffness are largely mitigated. It reduces the impact of individual components, such as columns and foundations, and shifts the optimal configuration for large-span buildings, where the articulated (pinned) system becomes the most sustainable option. These findings challenge the conventional preference for rigid connections in all contexts and demonstrate the adaptability of the composite approach when the full integrated structural system is considered. These results suggest that, for bare frames, composite typologies can be around 25–30 % less polluting over their life cycle compared to traditional systems, and this figure can rise to approximately 40–50 % for buildings with superstructures in which all components actively contribute to global performance.

Despite the significant advantages this novel composite typology offers, there remains substantial potential for further development and refinement of this framework. One key direction for future research is to apply optimization strategies to enhance structural robustness. Formulating the problem to explicitly consider performance objectives such as progressive collapse resistance [12] or fire resistance of steel girder elements [55] would allow the methodology to address not only environmental impact but also critical aspects of structural safety.

The proposed framework also shows strong potential for extension to more complex structural configurations. Future research should explore its application to irregular or asymmetric floor plans, as well as high-rise buildings, where the advantages of the composite system may become even more pronounced. The flexible grouping of design variables already embedded in the current approach allows for adaptation to diverse structural zones and varying load demands. Furthermore, while extreme wind actions in their static component have been included in the present study, additional work is needed to assess the system's behavior under dynamic and multi-hazard scenarios, such as earthquakes or fire coupled with structural degradation. Extending the optimization framework to address robustness under extreme conditions alongside life-cycle environmental impact would offer a more holistic understanding of the system's real-world potential and performance.

Another promising line of investigation is to use the developed optimization platform to explore alternative structural solutions, such as hybrid girders with web openings [56], steel–concrete composite systems (including slab–girder interaction) [15], or even systems based on engineered timber [20]. These comparative studies would allow for a broader evaluation of efficiency, enabling the construction industry to move toward increasingly sustainable and high-performance structural systems.

Other promising research lines are based on enhancing the precision and robustness of the LCA model. In more specific case studies, it is possible to define more accurate parameters, such as exact transport distances or site-specific environmental conditions. When detailed information is available, such as the type of protective coating system for steel elements, maintenance predictions can be refined accordingly. Deeper modeling approaches could include corrosion rate equations or experimental degradation curves to simulate time-dependent deterioration more realistically. Another promising direction involves incorporating the concrete cover thickness as an additional optimization variable, offering greater control over the durability and maintenance timelines of RC components [10]. Finally, evaluating how variations in key assumptions, such as concrete and steel recycling rates, affect life-cycle impacts would help assess the results' robustness and extend the proposed methodology's applicability. Deterministic frameworks, while useful for comparative purposes, may not fully capture the variability inherent in key parameters such as material properties, degradation rates, or maintenance intervals. To deal with these uncertainties, future research should also incorporate uncertainty-based approaches into LCA models [26,27]. Methodologies such as Reliability-Based Design Optimization (RBDO) or Robust Design Optimization (RDO) can be vital for linking uncertainty-based methods with optimization frameworks.

Formulating structural design optimization problems should evolve toward multi-objective approaches that address constructability, structural safety, and the specific performance of innovative components such as THVS girders (e.g., fire resistance or vibration). Applying the LHS-CINS methodology in a multi-objective context could help manage the increasing computational demands of more complex case studies, particularly when refining parameters such as the initial number of LHS solutions (N) to balance diversity and computational cost, or enhancing CINS variable-selection strategies. Surrogate-assisted optimization [7,12], replacing or complementing HFS with metamodels (or low-fidelity simulations), also offers a promising route to accelerate convergence without compromising solution quality.

To close this discussion, while this study focuses specifically on the structural component of the building, it contributes meaningfully to the broader goal of sustainable construction. The demonstrated potential to reduce environmental impact by 30 %, and up to 40–50 % when incorporating additional structural elements such as slabs and walls, highlights the significant role that structural optimization can play. However, achieving truly low-impact buildings requires a coordinated, multidisciplinary approach. Structural, mechanical, electrical, and environmental engineers and architects must each apply advanced design strategies, such as life-cycle assessment and artificial intelligence, to optimize their respective domains. Only through this integrated effort can the construction sector effectively reduce its environmental footprint and move closer to meeting global sustainability targets.

4. Concluding remarks

This study highlights the substantial benefits of applying Life-Cycle Environmental Impact Optimization (LCEIO) to structural design, focusing on the RC-THVS composite typology for frame buildings. This system integrates RC columns with Transversely Hybrid Variable Section (THVS) steel girders, offering a sustainable and efficient alternative to conventional RC frames.

Compared to conventional design, optimized composite systems reduce life-cycle impact by up to 32 %, with manufacturing-phase emissions lowered by up to 70 % due to superior material efficiency. Maintenance impacts decrease by ~45 %, driven by the girders' tapered geometry. Compared to optimized RC systems, the fixed-joint composite configuration achieves ~30 % lower emissions in low-aggressiveness environments, while in high-aggressiveness contexts it maintains a 21 % advantage, though reduced by increased steel maintenance demands. Under these harsher conditions, the pinned-joint configuration gains relative efficiency.

THVS girders also lower structural weight, reducing column and foundation demands. Parametric analyses show hybrid designs with

lower hybrid ratios than previous studies, using higher-quality steel webs, balance performance, and maintainability. Incorporating slabs and infill walls further reduces life-cycle impact by up to 42 %, making rigid joints ideal for small spans and pinned joints optimal for large spans with active secondary elements. These findings confirm that combining life-cycle optimization with strategic material and structural choices makes the RC-THVS system a highly sustainable alternative to traditional RC frames.

CRediT authorship contribution statement

Iván Negrin: Writing – review & editing, Writing – original draft, Visualization, Validation, Software, Methodology, Investigation, Formal analysis, Data curation, Conceptualization. **Víctor Yepes:** Writing – review & editing, Validation, Supervision, Resources, Project administration, Methodology, Funding acquisition, Conceptualization. **Moacir Kripka:** Writing – review & editing, Validation, Supervision, Methodology, Funding acquisition, Conceptualization.

Declaration of Competing Interest

The authors declare that they have no known competing financial interests or personal relationships that could have appeared to influence the work reported in this paper.

Acknowledgments

This work was supported by the Grant PID2023–150003OB-I00, funded by MICIU/AEI/10.13039/501100011033 and the European Regional Development Fund (ERDF), a program of the European Union (EU). Grant PRE2021–097197, funded by MICIU/AEI/10.13039/501100011033 and the European Social Fund Plus (ESF+), a program of the European Union (EU). Grant CNPq 305484/2023–0, funded by the Brazilian National Council for Scientific and Technological Development (CNPq).

Appendix A. Supporting information

Supplementary data associated with this article can be found in the online version at doi:10.1016/j.engstruct.2025.121461.

Data availability

Data will be made available on request.

References

[1] Luque-Castillo X, Yepes V. Life cycle assessment of social housing construction: a multicriteria approach. Build Environ 2025;282. https://doi.org/10.1016/j.buildenv.2025.113294.
[2] Esfandiari MJ, Urgessa GS, Sheikholarefin S, Manshadi SHDehghan. Optimum design of 3D reinforced concrete frames using DMPSO algorithm. Adv Eng Soft 2018;115:149–60. https://doi.org/10.1016/j.advengsoft.2017.09.007.
[3] Kaveh A, Rezazadeh Ardebili S. Optimum design of 3D reinforced concrete frames using IPGO algorithm. Structures 2023;48. https://doi.org/10.1016/j.istruc.2023.01.071.
[4] Mergos PE. Structural design of reinforced concrete frames for minimum amount of concrete or embodied carbon. Energy Build 2024;318. https://doi.org/10.1016/j.enbuild.2024.114505.
[5] Xiang Y, Mahamadu AM, Florez-Perez L, Wu Y. Design optimisation towards lower embodied carbon of prefabricated buildings: balancing standardisation and customisation. Dev Built Environ 2024;18. https://doi.org/10.1016/j.dibe.2024.100413.
[6] Zhang X, Zhang X. Automated component delivery management under uncertainty for prefabricated buildings to minimize cost and harmful emissions. Autom Const 2024;162. https://doi.org/10.1016/j.autcon.2024.105388.
[7] Negrin I, Kripka M, Yepes V. Metamodel-assisted meta-heuristic design optimization of reinforced concrete frame structures considering soil-structure interaction. Eng Struct 2023;293. https://doi.org/10.1016/j.engstruct.2023.116657.
[8] Negrin I, Chagoyén E. Economic and environmental design optimisation of reinforced concrete frame buildings: a comparative study. Structures 2022;38:64–75. https://doi.org/10.1016/j.istruc.2022.01.090.
[9] Lao WL, Li M, Wong BCL, Gan VJL, Cheng JCP. BIM-based constructability-aware precast building optimization using optimality criteria and combined non-dominated sorting genetic II and great deluge algorithm (NSGA-II-GD). Autom Const 2023;155. https://doi.org/10.1016/j.autcon.2023.105065.
[10] Negrin I, Kripka M, Yepes V. Multi-criteria optimization for sustainability-based design of reinforced concrete frame buildings. J Clean Prod 2023;425. https://doi.org/10.1016/j.jclepro.2023.139115.
[11] Ribeiro LR, Kroetz HM, Parisi F, Beck AT. Optimal risk-based design of reinforced concrete beams against progressive collapse. Eng Struct 2024;300. https://doi.org/10.1016/j.engstruct.2023.117158.
[12] Negrin I, Kripka M, Yepes V. Metamodel-assisted design optimization of robust-to-progressive-collapse RC frame buildings considering the impact of floor slabs, infill walls, and SSI implementation. Eng Struct 2025;325. https://doi.org/10.1016/j.engstruct.2024.119487.
[13] Hassan SA, Hanoon AN, Abdulhameed AA. Push-out test of eco-friendly steel-concrete–steel composite sections enhanced by polypropylene fibers: an experimental study and statistical analysis. Results Eng 2024;23. https://doi.org/10.1016/j.rineng.2024.102393.
[14] Lee D, Lim C, Kim S. CO_2 emission reduction effects of an innovative composite precast concrete structure applied to heavy loaded and long span buildings. Energy Build 2016;126:36–43. https://doi.org/10.1016/j.enbuild.2016.05.022.
[15] Brambilla G, Lavagna M, Vasdravellis G, Castiglioni CA. Environmental benefits arising from demountable steel-concrete composite floor systems in buildings. Resour Conserv Recycl 2019;141:133–42. https://doi.org/10.1016/j.resconrec.2018.10.014.
[16] Amin F, Ali I, Husnain A, Javed MF, Alabduljabbar H, Junaid A. Sustainable strengthening of concrete deep beams with openings using ECC and bamboo: an equation and data-driven approach through abaqus modeling and GEP. Results Eng 2025;26. https://doi.org/10.1016/j.rineng.2025.104813.
[17] Sabsabi A, Baalbaki O, Masri A, Ghanem H. Behavior of arch composite beam: experimental and numerical investigation. Results Eng 2025;26. https://doi.org/10.1016/j.rineng.2025.105076.
[18] Wang X, Zhuang B, Smyl D, Zhou H, Naser MZ. Machine learning for design, optimization and assessment of steel-concrete composite structures: a review. Eng Struct 2025;328. https://doi.org/10.1016/j.engstruct.2025.119652.
[19] Paksoy A, Aydogdu I, Akin A. Cost optimization of tall buildings having tube composite columns using social spider algorithm. Struct Des Tall Spec Build 2024. https://doi.org/10.1002/tal.2122.
[20] Shu Z, Zhou Y, Liu W, Li H, Li Z, Hu Q. Multi-objective optimization approach for timber-concrete hybrid shear wall building structures considering construction cost and carbon emissions. Structures 2025;78. https://doi.org/10.1016/j.istruc.2025.109221.
[21] Mela K, Heinisuo M. Weight and cost optimization of welded high strength steel beams. Eng Struct 2014;79:354–64. https://doi.org/10.1016/j.engstruct.2014.08.028.
[22] Negrin I, Kripka M, Yepes V. Design optimization of welded steel plate girders configured as a hybrid structure. J Constr Steel Res 2023;211. https://doi.org/10.1016/j.jcsr.2023.108131.
[23] Terreros-Bedoya A, Negrin I, Payá-Zaforteza I, Yepes V. Hybrid steel girders: review, advantages and new horizons in research and applications. J Constr Steel Res 2023;207. https://doi.org/10.1016/j.jcsr.2023.107976.
[24] Machado NB, Silvestre JD, Bohne RA. Embodied GHG emissions of reinforced concrete and timber structures: relevance, driving factors and target values. Build Environ 2025;275:112753. https://doi.org/10.1016/j.buildenv.2025.112753.
[25] Negrin I, Kripka M, Yepes V. Design optimization of a composite typology based on RC columns and THVS girders to reduce economic cost, emissions, and embodied energy of frame building construction. Energy Build 2025;336:115607. https://doi.org/10.1016/j.enbuild.2025.115607.
[26] Ping B, et al. Probabilistic life-cycle environmental impact of conventional and emerging steel frames in seismic zones. Earthq Eng Struct Dyn 2024;53:3113–39. https://doi.org/10.1002/eqe.4154.
[27] Ping B, Fang C, Hu Y, Yu S. Life-cycle cost assessment of conventional and self-centering steel frames in seismic zones: an extra focus on environmental impacts. Eng Struct 2025;325. https://doi.org/10.1016/j.engstruct.2024.119393.
[28] Fan J, Shao Y, Bandelt MJ, Adams MP, Ostertag CP. Sustainable reinforced concrete design: the role of ultra-high performance concrete (UHPC) in life-cycle structural performance and environmental impacts. Eng Struct 2024;316. https://doi.org/10.1016/j.engstruct.2024.118585.
[29] Wang J, et al. A novel life-cycle analysis framework to assess the performances of tall buildings considering the climate change. Eng Struct 2025;323(Part A):119258. https://doi.org/10.1016/j.engstruct.2024.119258.
[30] Heydari MH, Heravi G. A BIM-based framework for optimization and assessment of buildings' cost and carbon emissions. J Build Eng 2023;79. https://doi.org/10.1016/j.jobe.2023.107762.
[31] Su X, Huang Y, Chen C, Xu Z, Tian S, Peng L. A dynamic life cycle assessment model for long-term carbon emissions prediction of buildings: a passive building as case study. Sust Cities Soc 2023;96. https://doi.org/10.1016/j.scs.2023.104636.
[32] Chen H, Wang J, Shen QG, Chen B, Dong J, Feng Z, Liu Y. Application of hybrid machine learning algorithms for life cycle carbon prediction and optimization of buildings: a case study in China. Sust Cities Soc 2025;122. https://doi.org/10.1016/j.scs.2025.106248.

[33] Gao MY, Li C, Petzold F, Tiong RLK, Yang Y. Lifecycle framework for AI-driven parametric generative design in industrialized construction. Autom Const 2025; 174. https://doi.org/10.1016/j.autcon.2025.106146.
[34] Bao T, Lui Z. Evaluation of winkler model and pasternak model for dynamic Soil-Structure interaction analysis of structures partially embedded in soils. Int J Geomech 2020;20(2). https://doi.org/10.1061/(ASCE)GM.1943-5622.0001519.
[35] Klepikov SN. General solution for beams and plates on elastically deforming bases with varying stiffnesses. Bases, foundations and soil mechanics research. Kiev: Budivielnik; 1969. p. 37–47.
[36] International Organization for Standardization (ISO), ISO 14040: Environmental managment - life cycle assessment - principles and framework. Geneva, Switzerland, 2006.
[37] Penadés-Plà V, García-Segura T, Martí JV, Yepes V. An optimization-LCA of a prestressed concrete precast bridge. Sustainability 2018;10(3):685. https://doi.org/10.3390/su10030685.
[38] Navarro IJ, Villalba I, Yepes-Bellver L, Alcalá J. Social life cycle assessment of railway track substructure alternatives. J Clean Prod 2024;450. https://doi.org/10.1016/j.jclepro.2024.142008.
[39] Catalonia Institute of Construction Technology. BEDEC PR/PCT ITEC material database; 2016.
[40] Ciroth A. ICT for environment in life cycle applications openLCA — a new open source software for life cycle assessment. Int J Life Cycle Assess 2007;12:209–10. https://doi.org/10.1065/lca2007.06.337.
[41] Skoglund O, Leander J, Karoumi R. Optimizing the steel girders in a high strength steel composite bridge. Eng Struct 2020;221. https://doi.org/10.1016/j.engstruct.2020.110981.
[42] Huang Z, Zhou H, Tang H, Zhao Y, Lin B. Carbon emissions of prefabricated steel structure components: a case study in China. J Clean Prod 2023;406. https://doi.org/10.1016/j.jclepro.2023.137047.
[43] Wang L, et al. Energy consumption model of plasma spraying based on unit process life cycle inventory. J Mater Res TechnolJMRT 2020;9(6):15324–34. https://doi.org/10.1016/j.jmrt.2020.11.007.
[44] Hasan S, Bouferguene A, Al-Hussein M, Gillis P, Telyas A. Productivity and CO_2 emission analysis for tower crane utilization on high-rise building projects. Autom Constr 2013;31:255–64. https://doi.org/10.1016/j.autcon.2012.11.044.
[45] Ministerio de Transportes, Movilidad y Agenda Urbana, Código estructural, Boletín Oficial del Estado, (2021). [Online]. Available: ⟨https://www.transportes.gob.es/ministerio/normativa-y-estudios-tecnicos/reglamentacion-vigente-sobre-seguridad-estructural/codigo-estructural⟩.
[46] Tuutti K. CBI forskning research report. Corrosion of steel in Concrete. Stockholm, Sweden: Swedish Cem Concr Res Inst; 1982.
[47] García-Segura T, Yepes V, Alcalá J. Life cycle greenhouse gas emissions of blended cement concrete including carbonation and durability. Int J Life Cycle Assess 2014; 19:3–12. https://doi.org/10.1007/s11367-013-0614-0.
[48] Lagerblad B. Carbon dioxide uptake during concrete life-cycle: state of the art. Stockholm: Swedish Cement and Concrete Research Institute; 2005.
[49] L. Helsel, R. Lanterman, Expected Service Life and Cost Considerations for Maintenance and New Construction Protective Coating Work, Proceedings of the CONFERENCE 2024, New Orleans, LA, United States, pp. 1-15, https://doi.org/10.5006/C2024-20960.
[50] ISO 12944 (Parts 1–9). Paints and varnishes — corrosion protection of steel structures by protective paint systems. International Organization for Standardization (ISO); 2018.
[51] Akanbi LA, et al. Salvaging building materials in a circular economy: a BIM-based whole-life performance estimator. Resour Conserv Recycl 2018;129:175–86. https://doi.org/10.1016/j.resconrec.2017.10.026.
[52] World Steel Association, Life cycle assessment methodologies. ⟨https://worldsteel.org/steel-topics/life-cycle-thinking/life-cycle-assessment-methdologies/⟩, 2024 (accessed 27 December 2024).
[53] Abden MJ, Tam VWY, Afroze JD, Le KN. Energy efficient sustainable concrete for multifunctional applications. Constr Build Mater 2024;418. https://doi.org/10.1016/j.conbuildmat.2024.135213.
[54] Simon D. Biogeography-Based optimization. IEEE Trans Evolut Comput 2008;12 (6.):702–13. https://doi.org/10.1109/TEVC.2008.919004.
[55] Liu Y, Xu Q, Guo L, Wang J. Experimental and numerical study on the flexural performance of composite beams with channel-section steel girder under fire exposure. Eng Struct 2025;322(Part A). https://doi.org/10.1016/j.engstruct.2024.119059.
[56] Taş S, Erdal F, Tunca O, Ozcelik R. Effect of geometry on flexural behavior of optimal designed web-expanded beams. J Constr Steel Res 2024;215. https://doi.org/10.1016/j.jcsr.2024.108500.